

2009-2010 Hydraulic Dynamometer

A Major Qualifying Project
Submitted to the faculty of
Worcester Polytechnic Institute
In partial fulfillment of the requirements for the
Degree of Bachelor of Science

Submitted By:

Robert McNamee

Ian Monk

Thomas Page

Michael Taglieri

Approved:

James D. Van de Ven, Advisor

Date: April 29th, 2010

Abstract

This report describes the design and construction of a hydraulic dynamometer as a research tool for testing engines and transmissions for the Mechanical Energy and Power Systems (MEPS) laboratory. A literature review was conducted to understand hydraulics, dynamometers, and data acquisition systems (DAQ), which was followed by a complete design of a hydraulic system. This dynamometer has both active and passive cycles. In both modes the dynamometer tests a machine under test (MUT) that drives a hydraulic pump/motor. A proportional valve imparts a load on the MUT by restricting flow and creating a pressure differential. A fluid conditioning loop comprised of a heat exchanger and filter is incorporated into the return line. In the active cycle the dynamometer can simulate regenerative braking using an external power source to create a flow at the inlet of the main pump/motor. This flow allows the MUT to do less work to pull the oil through the system. In the passive cycle the dynamometer is only absorbing energy and measuring power. There is a flow control valve prior to the main pump to switch between modes. Based on this design, a successfully functioning system was constructed. This project combined different disciplines including mechanical, manufacturing, systems, and electric and computer engineering to provide a tool to aid in future research within the MEPS laboratory.

Acknowledgements

We would like to thank:

- National Fluid Power Association for financial support of this project
- Adam Allard, US Hydraulics, Manchester NH
- Professor James Sullivan (WPI)
- Neil Whitehouse (WPI)
- Professor James O'Rourke (WPI)
- Randy Robinson (WPI)
- Professor James D. Van de Ven (WPI project advisor)

Table of Contents

Abstract	i
Acknowledgements	ii
Table of Contents	iii
Table of Figures	v
Table of Tables	vii
Introduction	1
Background	3
Dynamometers	3
Regenerative Braking	5
Hydraulics	5
Goal Statement	15
Task Specifications	16
System Design and Manufacturing	17
Selection of Hydraulic Circuit	17
Individual Component Selection	22
Design and Manufacturing of the Components	28
System Layout	32
Data Acquisition and Controls	36
Pressure Calculations	36
Torque	37
Proportional valve	39
Directional Control Valve and Electric Motor	41
Angular Velocity	41
Experiment Set Up	43
Selection of DAQ Device	43
Individual Components	44
Calculations within Experiment	49
Active and Passive Cycle	50
Recording the Data	51
Benefits of the Experiment	51
User Interface	52

Final Testing	55
Calibration	55
Remaining Components.....	57
Results.....	57
Future Recommendations	60
Load Cell.....	60
Dampening Vibrations	60
References.....	61
Appendix A: Sizing of Hydraulic Pump.....	62
Appendix B: Reservoir	64
Appendix C: Heat Exchanger	65
Appendix D: Cradle	69
Appendix E: Torque Arm	74
Appendix F: Stress Calculations.....	76
Appendix G: Manifold.....	77
Appendix H: Heat Exchanger	78
Appendix I: Base Plate.....	80
Appendix J: Strain Gage Calibration	81
Appendix K: Results	85

Table of Figures

Figure 1: Simple Hydraulic Dynamometer Schematic	4
Figure 2: EPA Driving Schedule	4
Figure 3: External Gear Pump	6
Figure 4: Gerotor Pump	7
Figure 5: Vane Pump	8
Figure 6: Axial Piston Pump.....	8
Figure 7: Radial Piston Pump	9
Figure 8: Key for Circuit Diagrams	17
Figure 9: Hydraulic Circuit, Idea 1	18
Figure 10: Hydraulic Circuit, Idea 2.....	18
Figure 11: Hydraulic Circuit, Revision B.....	19
Figure 12: Hydraulic Circuit, Revision C.....	19
Figure 13: Hydraulic Circuit, Revision D.....	19
Figure 14: Hydraulic Circuit, Revision E	20
Figure 15: Hydraulic Circuit, Revision F	20
Figure 16: Hydraulic Circuit, Revision G.....	21
Figure 17: Sun Hydraulics FPCH proportional valve schematic.....	23
Figure 18: Pressure vs. flow curves for directional control valve	24
Figure 19: Unmodified control valve schematic.....	24
Figure 20: Schematic with "Port B" blocked.....	24
Figure 21: Main Pump/Motor Cradle	29
Figure 22: Torque Arm	30
Figure 23: Top level of cart	34
Figure 24: Bottom level of cart.....	34
Figure 25: Entire System	35
Figure 26: Instrumentation Amplifier.....	38
Figure 27: Block diagram representation of proportional valve PID controller.....	39
Figure 28: PWM duty cycles	40
Figure 29: PWM Circuit	41
Figure 30: Creation of Virtual Channel for Pressure Transducer.....	45

Figure 31: Calculations for Pressure Transducer	45
Figure 32: Creation of Virtual Channel for Electric Motor	46
Figure 33: Generation of the Signal for the Electric Motor	46
Figure 34: Creation of Virtual Channel for Control Valve	47
Figure 35: Generation of the Signal for the Control Valve	47
Figure 36: Creation of Virtual Channel for the Proportional valve	47
Figure 37: Generation of the Signal for the Proportional valve.....	48
Figure 38: Creation of Virtual Channel for the Strain gage.....	48
Figure 39: Computing the Strain gage Signal.....	48
Figure 40: Creation of the Virtual Channel for the Hall Effect Sensor	49
Figure 41: Reading the Data of the Hall Effect Sensor	49
Figure 42: Formula Node for Power Calculation	49
Figure 43: PID Controller Feedback Loop	50
Figure 44: User Control to Switch Between Active and Passive Cycles.....	51
Figure 45: Active and Passive Cycle Loop.....	51
Figure 46: User Interface - Basic	53
Figure 47: User Interface - Advanced.....	54
Figure 48: Results for Diesel Engine	58
Figure 49: Horsepower of MUT	59

Table of Tables

Table 1: Causes of Cavitation and Aeration	10
Table 2: Causes of Internal Contamination	12
Table 3: Components and Channels Necessary	44
Table 4: Channel Types and Amount on NI PCI-6221.....	44
Table 5: How to Interpret LabVIEW Block Diagram	45

Introduction

At Worcester Polytechnic Institute's Mechanical Energy and Power Systems (MEPS) laboratory, research is being conducted on alternative power systems. This research includes the development of a number of unique engines and drive trains. Currently, there are no laboratory devices to test or validate the characteristics of these systems, limiting the research capabilities of the laboratory.

The goal of the project is to design and construct a portable hydraulic dynamometer to test a variety of research engines and transmissions, and to simulate the regenerative braking cycle of a scaled hybrid vehicle drive train. To achieve this goal, the hydraulic dynamometer must be a universal dynamometer; meaning that it can both generate and absorb power. The system must also accurately measure the output torque and angular velocity of the machine under test (MUT).

This project is guided by constraints in three categories: performance constraints, design constraints, and project constraints.

Performance constraints are focused on the power generation of the system, absorption of the energy produced by the MUT, evaluations of the MUT outputs, and safety. First, the MUT's torque characteristics must be defined as a function of angular velocity. The system must absorb that power in a safe manner across the entire speed range. At the same time, the hydraulic circuit must be designed to switch from a passive cycle (absorbing power) to an active cycle (generating power) safely and easily. Finally, the energy dissipated as heat must be removed from the system.

Design constraints include aspects such as portability. The system must be transportable by one person between experimental locations. It was determined that the components of the system would have to be run by a typical wall outlet. Additionally, the components had to be sized to avoid possible problems such as cavitation. Project constraints are the four term completion schedule.

In this report the background will first be developed to give the user an introduction into some the important aspects of dynamometers, regenerative braking and hydraulics. This is followed by the task specifications and the layout of the system then by the methodology of how components were selected and/or manufactured. The final portion of the methodology includes

the design of the electrical and data acquisition systems. The paper concludes with the results from final testing as well as recommendations for future improvement.

Background

The background section explains important prerequisite information about aspects of the project. It gives the reader information regarding dynamometers, regenerative braking, and hydraulics.

Dynamometers

A dynamometer is a mechanical device that measures the torque of a given MUT. Two basic classifications of dynamometers are absorption (passive) and universal (active). Passive dynamometers are driven or motored by the given input. The active dynamometers can drive the system as well as be driven. With numerous applications, they have been employed in areas ranging from the medical field for monitoring the muscle strength of healing limbs, to the automotive field for examining the torque outputs of engines and drive trains at different angular velocities [5]. For the purposes of this project, the focus will be on the dynamometers that measure the torques of engines and drive trains.

A common dynamometer in use in industry is the engine dynamometer where it is connected to the crankshaft of the engine. The dynamometer then applies a resistance, or load, to the engine at different angular velocities. The load can be applied by using a variety of brakes including an electric brake, water brake, or friction brake. Figure 1 demonstrates a simple schematic of this process. In this system, the dynamometer is seated in bearings, allowing it to rotate. This rotation is prevented by a torque arm with an attached force-measuring scale, generally a strain gage. As the dynamometer loads the engine, the torque arm experiences a force. This force multiplied by the distance from its center of rotation equals the torque of the engine. With the known torque and angular velocity, the power of the system can be calculated from the product of these two values. The purpose of the engine dynamometer is to examine the engine's performance. These systems are generally universal, so that the performance can be analyzed by driving the load and being driven by the load; the passive and active cycles, respectively [5].

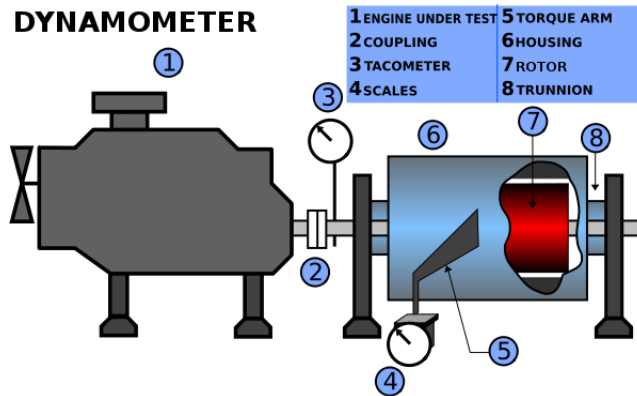


Figure 1: Simple Hydraulic Dynamometer Schematic
<http://en.wikipedia.org/wiki/File:Dynamometer01CJC.svg>

A chassis dynamometer is similar to an engine dynamometer, but collects its data through the vehicle's tire rotation. These tests can be performed to evaluate the fuel efficiency of the vehicle under different simulate situations. For example, Figure 2 shows an EPA driving schedule, which simulates a vehicle subjected to driving conditions in an urban area. At any of these points in time on the graph, the dynamometer can vary the load to simulate a hill and the vehicle's ascent or descent. Other suggested driving schedules simulate highway driving and heavy duty vehicle urban driving (EPA).

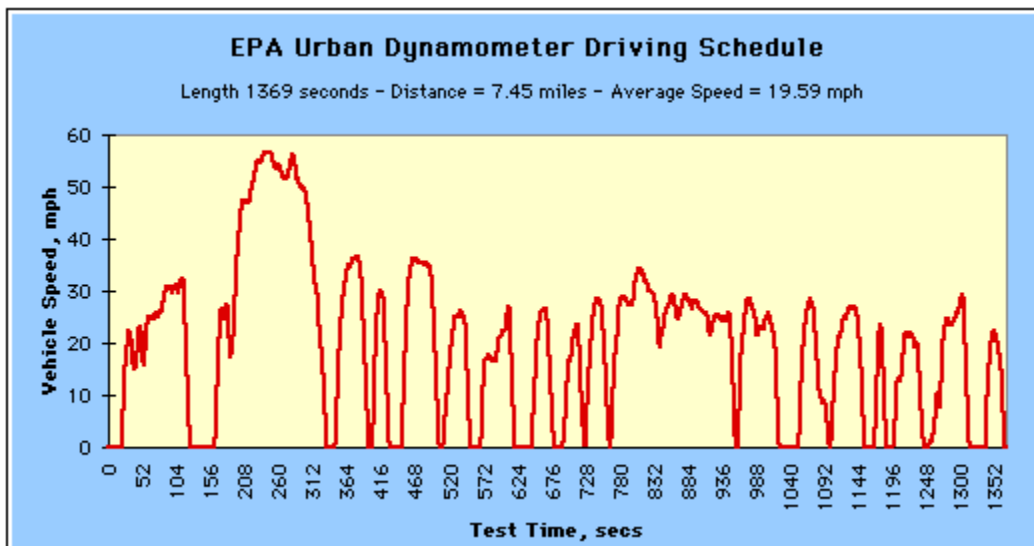


Figure 2: EPA Driving Schedule
<http://www.epa.gov/nvfel/methods/uddsdds.gif>

Regenerative Braking

Hydraulic systems prove to be efficient for hybrid vehicle applications due to their high power to weight ratio. For example, consider the system called Hydraulic Power Assist (HPA), developed by the Ford Motor Company and Eaton Corporation. During the braking process, a hydraulic pump is used to absorb the vehicle's kinetic energy as it slows. The hydraulic fluid displaced by the pump enters a storage reservoir, the hydraulic accumulator. The hydraulic fluid compresses a gas in the hydraulic accumulator, storing energy and slowing the vehicle. When the vehicle begins acceleration, the pump can be reversed and the accumulators will help supply energy. It is stated that this system can store 80% of the vehicles lost momentum [4].

Another form of regenerative braking, popular in hybrid vehicles, uses electric energy storage. As the vehicle brakes, the wheels drive an electric motor/generator to charge a battery. This battery releases the stored electricity when the accelerator is reapplied and become the driving agent. This is similar to the hydraulic braking system where the accumulator can be equated to the battery and the pump to the electric generator [4].

Hydraulics

Hydraulics is the application of converting mechanical energy using an incompressible fluid and returning it to mechanical work. There are several important advantages of hydraulic systems, including variable speed, rapid reversibility, high control bandwidth, and high power to weight ratios.

Types of Hydraulic Pumps

Hydraulic pumps convert mechanical energy into hydraulic energy by moving high pressure fluid through a system. Generally, the pump is the primary flow control device in any circuit and most pumps work on the same principle. They generate a flow by sucking fluid in at the inlet and discharging at a higher pressure at the outlet. The hydraulic horsepower from a pump is determined by the flow provided by the flow rate and the operating pressure [2]. A common formula used is:

$$\text{Hydraulic Horsepower} = \text{Pressure (Pa)} \times \text{Flow} \left(\frac{m^3}{min} \right)$$

Positive displacement pumps can be classified into two categories: fixed displacement pumps and variable displacement pumps. In fixed displacement pumps the pump delivers a fixed

volume of fluid for each revolution. This is defined as the displacement of the pump and is usually reported as in^3/rev . Variable displacement pumps are designed so that the output of fluid per revolution can be changed while the pump is operating.

Fixed Displacement Pumps

Fixed displacement pumps have a displacement that cannot be changed without replacing some internal components of the pump. Gear pumps are only available with a fixed displacement. These pumps are less expensive and thus widely used. The leakage in some gear pumps is high, and this leakage will increase as the pump wears over time [2].

An external gear pump is shown in Figure 3. One gear, called the drive gear, is driven with the input shaft, which drives the second gear, known as the driven gear. As the gears mesh, a partial vacuum is created, allowing fluid into the spaces between the teeth. As the gears rotate, the fluid is carried around the housing to the outlet. The fluid cannot return to the inlet because the spaces between the teeth are already filled with the meshing gear teeth. The design is simple and inexpensive. It is apparent there are opportunities for leakage all along the housing. The displacement for these types of pumps is between 1 cm^3 and 200 cm^3 . Gear pumps are popular for their simplicity and robustness [2].

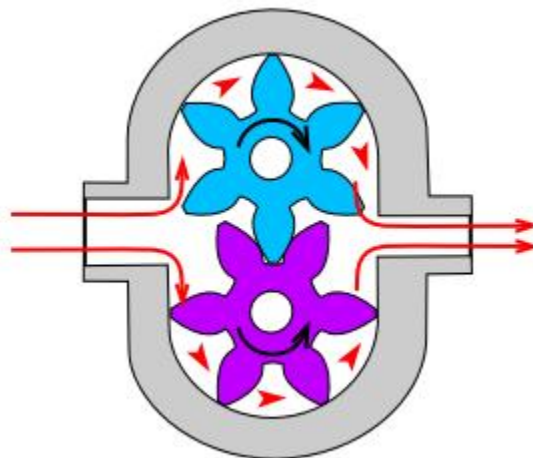


Figure 3: External Gear Pump

<http://ihpv.free.fr/myihpv/possibilities/hydrostatique/HydraulicGearPump1.png>

A gerotor (gear) pump, one of the most common internal gear pumps, as seen in Figure 4, has an inner drive gear and an outer driven gear. The inner drive gear has one less tooth than the

driven gear. As the inner gear rotates it drives the outer gear. Chambers of decreasing volume are created between the gear teeth, and thus creating a pumping action [2].

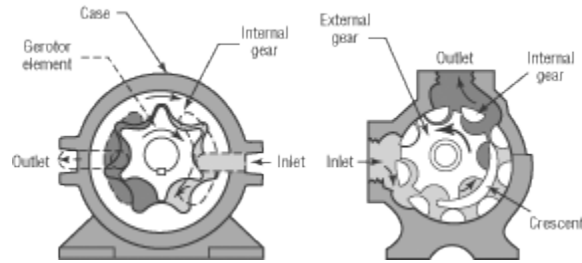


Figure 4: Gerotor Pump

http://www.hydraulicspneumatics.com/FPE/images/pumps1_4.gif

Although they are fixed displacement pumps, there are two ways gear pumps can provide altering flow rates. The first is to change the dimensions of the gears by replacing the existing ones with new ones. The second is by varying the speed at which the drive gear turns [2].

Variable Displacement Pumps

Unlike fixed displacement pumps, variable displacement pumps are able to generate varying displacements, as the name implies. These are more versatile than a fixed displacement pump because by changing the displacement the characteristics of the circuit are changed by varying the flow. However, these pumps are generally more expensive than a fixed displacement pump.

Vane Pump

A vane pump as seen in Figure 5 has a series of vanes that slide back and forth in slots. There are springs in these slots that push the vanes out until the tip contacts the cam ring. A chamber is formed between adjacent vanes and the cam ring. As the rotor turns, the chamber decreases in volume. Fluid flows into the chamber when at its maximum and out when it is at its minimum. This change in chamber size creates the pumping action [2].

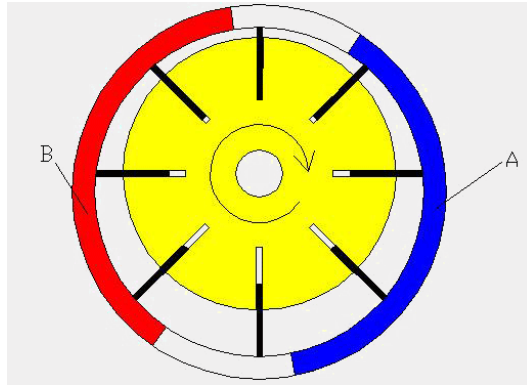


Figure 5: Vane Pump

http://www.tenderliftsandcranes.com/images/img_gear_pumps_3.gif

Axial Piston Pump

An axial piston pump, as shown in Figure 6 has a series of cylinders mounted parallel to the axis of rotation. Pistons are inserted into the cylinders with their spherical ends mounted in a shoe. The shoe is held against a swash plate by a spring in the cylinder block. When the swash plate is at an angle to the shaft it moves the pistons back and forth in the cylinders as the entire cylinder block rotates. If constructed properly, the fluid will flow into the cylinder during the first 180° of rotation, then will be forced out during the final 180° of rotation [2].

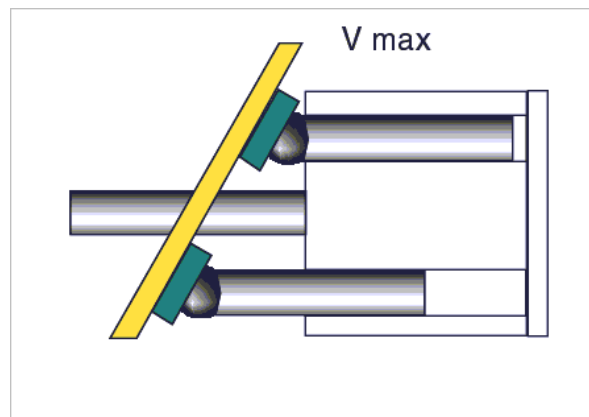


Figure 6: Axial Piston Pump

Radial Piston Pump

A radial piston pump as shown in Figure 7 is similar to an axial piston pump, except the cylinders are mounted radially around the axis of rotation. As the shaft rotates, the connecting rods push the pistons back and forth in the cylinders, developing the pumping action. These are used for high pressures and small flows. Normally pressures up to 650 bar [2].

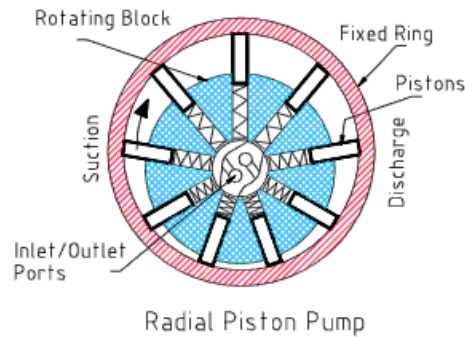


Figure 7: Radial Piston Pump

Aeration and Cavitation

Aeration and cavitation are two phenomena that frequently cause pump failure. Aeration is caused by air entering the system and is most destructive when passing through the pump. Cavitation is usually caused by inadequate pump inlet conditions, and is equally destructive. Both are noisy and must be corrected as quickly as possible when identified [3].

Aeration

Aeration occurs when air enters the inlet of the pump along with hydraulic fluid. The air enters either from a leak in the inlet lines or due to low fluid levels in the reservoir. Air can also be mixed with the fluid returning from the hydraulic system or from turbulence in the reservoir. The low pressure at the inlet causes the air bubbles to expand. When the fluid is pressurized the bubbles collapse. This causes an implosion and will release large amounts of energy as each bubble forms a micro jet. This will cause rapid erosion of the internal pump components [3].

Cavitation

The difference between cavitation and aeration is that the vapor bubbles form in the fluid at the inlet, rather than the fluid already having air in it as it approaches the inlet. The bubbles form at the inlet due to excessively low inlet pressure for the fluid being used. Once in the pump the bubbles cause the same damage as aeration. A common cause for cavitation is a restriction in the flow of the hydraulic fluid to the inlet of the pump. Table 1 shows the causes of aeration and cavitation [3].

Table 1: Causes of Cavitation and Aeration

Causes of Cavitation	Causes of Aeration
Clogged or restricted strainer	Low reservoir fluid level
High fluid viscosity	Defective pump shaft seal
Low fluid temperature	Return line above fluid level
Clogged reservoir breather	Improper baffling in the reservoir
Pump inlet line too small	Loose fitting on pump inlet
Pump too far above reservoir	Defective seal on pump inlet
Pump too far from reservoir	Incorrect reservoir design
Too many binds in pump inlet line	
Collapsed hose n pump inlet line	
Restriction on pump inlet line	
Failure of supercharge pump	

Temperature Control

Operating temperatures consistently above 160°F promotes chemical reactions that change the properties of hydraulic fluid. Effects of high temperature include: oxidation of the oil, formation of insoluble gums, varnishes and acids, deterioration of seals, loss of lubricity and changes in viscosity [3].

The gums and varnishes clog orifices and cause valves to stick. The acid attacks the metal surfaces and causes corrosion. The most significant effect of high temperature is the reduction in viscosity and thus the reduction in lubricity. At some point metal-to-metal contact occurs, and damage results. It is recommended that hydraulic systems be designed to operate at a temperature less than 140°F under worst case ambient conditions [3].

Methods for Cooling Hydraulic Oil

Since no system can ever be 100 percent efficient, heat is a common problem. Two types of heat exchangers are used to cool hydraulic oil: Shell-and-tube and finned tube. The shell-and-tube is an oil to water exchanger while the finned tube is an oil-to-air exchanger. The shell and tube has a series of tubes inside a closed cylinder. The oil flows through the small tubes, and the

fluid receiving the heat (water) flows around the tubes. These exchangers can be single pass or double pass [2]

Air coolers such as the finned tube exchanger are commonly used when water is not available for cooling. In a finned tube exchanger the fluid is pumped through tubes that are bonded to fins that transfer heat to the outside air. A fan is often added to the cooler to increase the heat transfer. Air coolers are less efficient than water coolers and tend to be less effective when ambient temperatures are high. The installation cost are higher than water coolers, however the operational costs are typically less [3].

Contamination Control

There is a great deal of knowledge about the prevention and control of contaminate buildup. Despite this knowledge it is estimated that over 80% of hydraulic system failures are due to poor fluid condition. A contaminate is any material in a hydraulic fluid that has a harmful effect on the fluid's performance in a system. Simply stated, a contaminate is any foreign substance that causes harm to the hydraulic or lubrication fluid of a system. They can be gaseous, liquid or solid [3].

Types of Contamination

There are four sources of contamination in hydraulic fluids.

- 1) Built in contamination: Contaminate that was left in the system when it was constructed.
- 2) Contaminated new oil: Contaminate that is introduced during the manufacturing and handling of oil.
- 3) Ingressed Contamination: Contaminates that are introduced into the system from the environment. Contaminates enter along with air flowing into the reservoir through the breather cap, or into the cylinder rod. Also if the system is opened in any way there is a chance for contamination to ingress. Can also occur during servicing or maintenance.
- 4) Internally generated contamination: Particles removed from the internal components can circulate within the system until they are removed. This is also known as wear generation cycle. Table 2 shows the type and cause of some internally generated contaminants [3].

Table 2: Causes of Internal Contamination

Type	Cause
Abrasion	Particles grinding between moving surfaces
Erosion	High velocity particles striking surfaces
Adhesion	Metal-to-metal contact
Fatigue	Repeated stressing of a surface
Cavitation	High pump inlet vacuum
Corrosion	Foreign Substance in fluid
Aeration	Gas bubbles in fluid, introduced air to pump inlet

Effects of Contamination

Solid contamination interferes with power transmission by blocking or plugging small orifices in devices such as valves. A valve affected in this manner is unpredictable and unsafe. Contamination can also form sludge on the reservoir walls and interfere with the cooling process. This will cause the operating temperature to increase [3].

The most serious effect contamination has on the system is the loss of lubrication. This can occur in several ways. Particles can collect in mechanical clearances and block the flow of lubricating fluid into the spaces between moving parts. This is known as silting. Silting can cause valves to shift improperly, degrade pump performance and add heat to the system by reducing pump efficiency [3].

The effects of contamination on the pump are especially of concern. It is an expensive component with many surfaces that can be scarred, eroded, or chemically altered. The operating life cycle of most pumps is determined by the removal of very small quantities of material. Contamination can cause leakage to increase through enlarged clearances, operating temperatures to go up, chemical reactions between the metal and fluids to increase, which all cause pump performance to degrade [3].

Controlling Contamination

The main component for controlling contamination is a filter. The main goal of filtration is to prevent the ingress of contaminant. All air entering the reservoir needs to be filtered as it is much easier to remove contaminants from the air rather than the fluid. All fluid enter the

reservoir must be filtered as well. The best way to do this is with a transfer cart. This has a pump, filter and supply of fluid. The pump pumps fluid into the reservoir through the filter, thus capturing any contaminate in the replacement fluid prior to entering the reservoir. There are three areas in hydraulic systems for locating a filter: the pressure line, the return line and an off-loop or kidney loop type filtration circuit [3].

Pressure Line Filters

A pressure line filter is considered the “gateway” contamination control device for a system. However, it does not protect the pump from any contamination that is returned to the reservoir from the system. Pressure line filters should not be used alone and should always be used in servo or proportional valve systems to protect these products from any wear particles that may be generated by the pump during operation [3].

There are a number of filters designed for installation in the pressure line. This type of filter might be used where system components are less dirt tolerant than the pump or to protect downstream components from pump generated contamination. Pressure line filters must be able to withstand the operating pressure of the system as well as the pump pulsations [3].

Return Line Filters

Return line filters are a total system contamination control device. They can also trap small particles before the fluid returns to the reservoir. Return line filters are most effective when at least 20 percent of the total system volume passes through the filter every minute. They are necessary in a system with high performance components which have very close clearances. Care must be taken to size the return line filter for the maximum flow it will experience. If the return line filter is not sized properly, it could rupture, contaminating the fluid in the reservoir. Full flow return filters should have enough capacity to handle maximum return flow with minimal pressure drop. Full flow means that all the flow generated by the system will pass through the filtering element [3].

Off-Line Filter Systems

Filter performance is optimized during steady flow, relatively free of pressure fluctuations. This is one tradeoff for pressure and return line filters. One way to optimize filter performance is to replace the filter in the main system with an independently powered re-circulating system where the filter is subjected to fewer variables. Off –line filter systems are

desirable when operating conditions are severe and the necessary quality of filtration within the system is difficult to obtain [3].

An off-line circulating pump should always be used when a pressure-compensated system is on standby for long periods of time. During standby, fluid is not passing through the pressure or return line filters, and pump generated contamination is passing directly into the reservoir. The off-line system will clean the fluid during this phase. It can also be run before starting the system to clean the fluid in the reservoir and reduce the level of contamination during start-up. Off-line filter systems can be placed in the system where it is convenient for servicing [3].

Reservoirs

Reservoirs serve several functions besides holding the system fluid supply. By transferring waste energy through its walls, the reservoir acts as a heat exchanger. The reservoir also allows entrained air to rise and escape while solid contaminants settle to the bottom, acting as an aerator and fluid conditioner. These are functions that can also be provided to the system by methods that do not involve the reservoir. The reservoir may also be used as a platform to support the pump, motor, and other components, saving floor space [3].

A large tank is desirable to promote cooling and separation of contaminants. At a minimum the tank must be large enough to hold all the fluid in the system and maintain a high enough fluid level to prevent a whirlpool effect at inlet opening. A whirlpool effect at the inlet opening will cause aeration. For industrial use a general sizing rule is used [1]:

$$\textit{Tank size(liters)} = \textit{pump liters/ min} \times 2 \textit{ or } \times 3$$

Goal Statement

The goal of this project was to design and construct an active hydraulic dynamometer to be used as a test bed for various engines and drive trains as well as simulate the regenerative braking cycle of scaled hybrid vehicles.

Task Specifications

Task specifications were created to specify the needs of the system. Task specifications include performance specifications as well as design specifications.

- 1) Must be safe to operate
- 2) Must have a passive cycle (apply a load to the test engine)
- 3) Must have an active cycle which simulates a regenerative braking cycle
- 4) Must operate at a max torque of 20 N•m and from 0-3800 rpm during the passive cycle
- 5) Must be able to connect to the hydraulic power unit
- 6) Measure torque and angular velocity within 0.5% accuracy
- 7) Must be adaptable to different engines/drive-trains with a foot print of 1.5 ft x 1.5 ft
- 8) Must automatically plot output variables (torque, angular velocity) vs. time
- 9) Must maintain working fluid temperature < 140°F
- 10) Must be able to switch between active and passive cycles with push of one button
- 11) Must be operable by a single person
- 12) All components must be computer controlled
- 13) Operate off of 110 V 20 amp circuit
- 14) Must contain a built in data acquisition system

System Design and Manufacturing

Once a clear scope of the project was established and task specifications determined, the detailed design of the dynamometer began. The first step was to create a hydraulic circuit that incorporated both an active and passive cycle. Hydraulic components were then properly sized and purchased to meet our maximum system operating ranges as outlined in the task specifications. Finally, custom parts were designed, manufactured and placed on the cart. The following sections describe how each of these steps was accomplished.

Selection of Hydraulic Circuit

The selection of an efficient and operable hydraulic circuit design has proven to be an iterative process. Generating both an active and passive cycle while still allowing for accurate measurement readings has been a main driving factor. Several preliminary circuits were designed and the positive and negative attributes of each were discussed, and a final selection was made. With the selected hydraulic circuit, sizing of components and further analysis was performed. Figure 8 shows a key which can be used for the following diagrams.

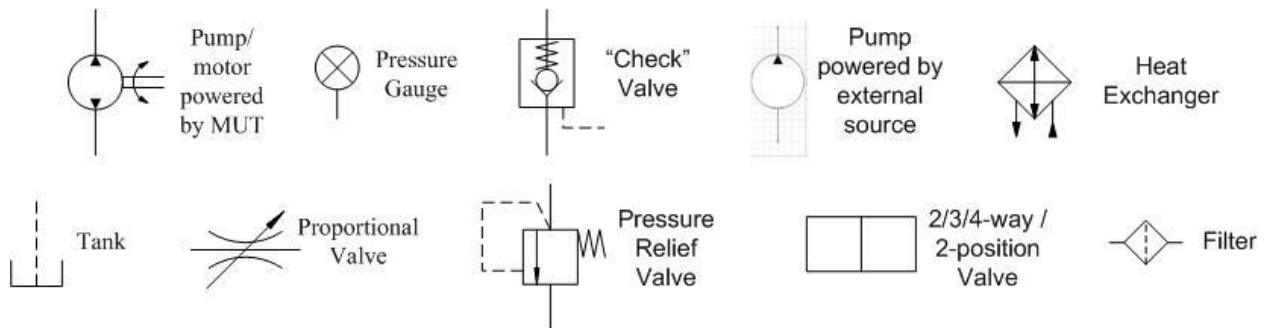


Figure 8: Key for Circuit Diagrams

Preliminary Ideas

Two preliminary ideas were discussed in order to accomplish the goal of designing the hydraulic dynamometer circuit. The preliminary design ideas can be seen in Figure 9 and Figure 10. These circuits were crude and demonstrate the initial lack of experience in the subject matter. Although these systems look different schematically, the systems share many similarities. Both circuits utilize a 4-way/2-position valve to toggle the system between the active and passive cycles. Additionally, they both include the use of a restrictor valve to create pressure gradients, pressure relief valves for safe operation, and pumps powered by electric

motors to simulate the active cycle of the system. The main differences are in their complexity and the different valves used to accomplish tasks.

It was decided that the design, which can be seen in Figure 9, was the most practical choice. This decision was based on ease of manufacturing, cost, and efficiency due to fewer valves. However, future iterations would be needed because this system still had many flaws, such as, no documented way to calculate power and not enough relief valves. With this selection, the iteration process continued.

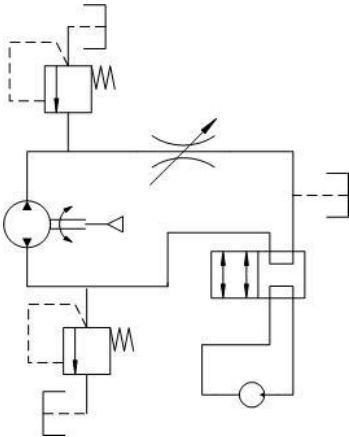


Figure 9: Hydraulic Circuit, Idea 1

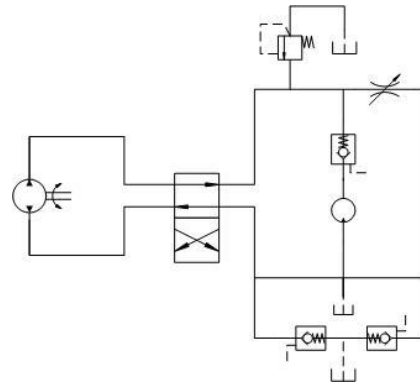


Figure 10: Hydraulic Circuit, Idea 2

Optimization of the Hydraulic Circuit

Figure 9 depicts the preliminary design again and changes can be seen in Revision B, shown in Figure 11. The major difference between the first and second iteration is the addition of pressure gauges on either side of the proportional valve. These are a crucial part to the system as it was originally intended to measure the pressure gradient (ΔP) across the proportional valve to calculate power of the MUT. Other minor changes include the addition of various safety features including an additional line to tank after the 2 position valve, which would help minimize the possibility of cavitation of the oil in the active cycle. An on/off valve was also added to minimize the possibility of cavitation in the passive cycle. Future revision was still needed because this iteration was still very crude and could be better optimized, such as placing pressure relief valves in more appropriate areas.

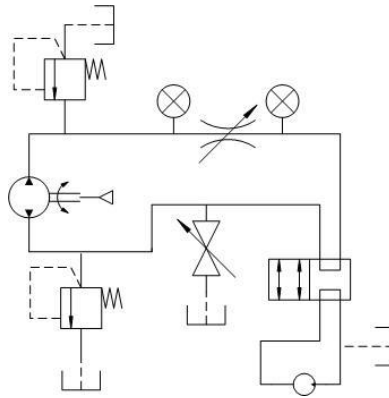


Figure 11: Hydraulic Circuit, Revision B

Minor changes were also made between Revisions B and C (Figure 11 and Figure 12 respectively), but the major changes can be seen between Revisions C and D (Figure 12 and Figure 13 respectively). The 4-way/2-position valve was modified into a 2-way/2-position valve. In the passive cycle, the proportional valve would still create a pressure drop across itself and ΔP could be measured, but the line would then dump straight to tank. The on/off switch which is depicted just below the pump in Figure 13 would be toggled into the ‘on’ position allowing the pump to draw from tank, resulting in a fully connected circuit. In the active cycle, the on/off switch would be toggled ‘off,’ the 2-way/2-position valve would be switched to the second position, and the pump powered by the electric motor would be turned on. The proportional valve would create a pressure drop and then return to tank. This pressure would remain constant until it arrived at the MUT pump/motor where the high pressure fluid would apply a negative torque to the motor thus simulating the regenerative braking cycle.

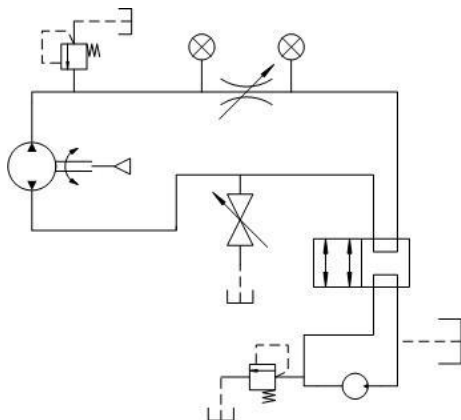


Figure 12: Hydraulic Circuit, Revision C

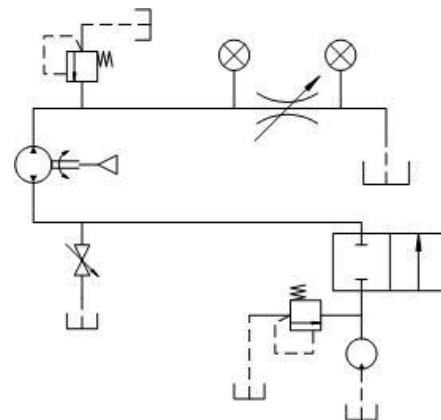


Figure 13: Hydraulic Circuit, Revision D

It was noticed that the on/off valve could be eliminated by simply creating a 3-way/2-position valve; this modification

can be seen between revisions D and E (Figure 13 and Figure 14 respectively). The major differences between revisions E and F are the locations where measurements are to be taken. It was originally determined to calculate the power of the MUT using the following equation:

$$Power = Flow * \Delta P$$

Measuring power by multiplying flow by the pressure change, although correct, is difficult to accurately measure due to the volumetric and mechanical efficiency of the pump. Therefore, it was determined to measure the power using the following equation:

$$Power = Torque * Angular Velocity$$

With this being agreed upon, two pressure gauges were no longer needed. However, due to safety concerns as well as this system being used in academic purposes, one pressure gauge would be left on the system placed immediately before the proportional valve where the pressure would be highest. Not depicted in Figure 15 is the process which will be used to measure the torque or angular velocity. The torque will be measured by developing a cradle to hold the motor in bearings allowing it to be free to rotate. Attached to this cradle will be a torque arm where strain gages will be mounted allowing the torque to be recorded; the angular velocity will be recorded using a Hall-effect sensor. Both of these processes will be discussed in far greater depth in later sections of the report.

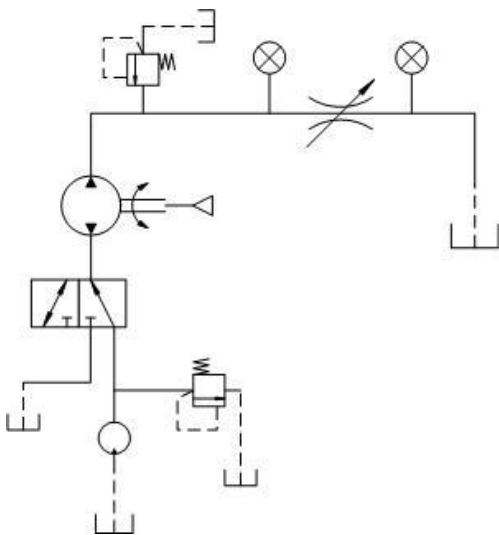


Figure 14: Hydraulic Circuit, Revision E

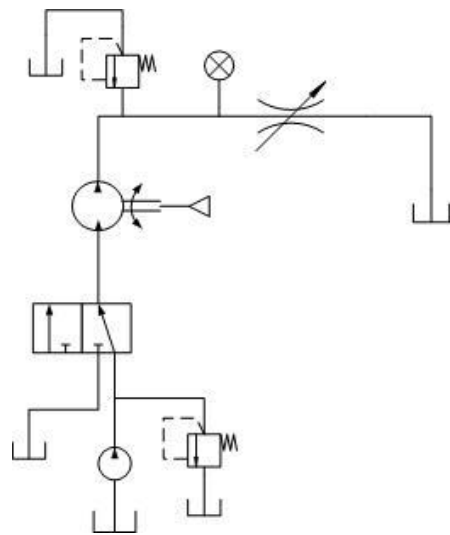


Figure 15: Hydraulic Circuit, Revision F

The final revision can be seen in Figure 16. The general layout of the system is identical, but some more detail has been added. A heat exchanger has been added to the system to assure that it will continuously run at an appropriate temperature.

The way which the final circuit will function is now described. The view shown in Figure 16 depicts the passive cycle as the 2-position valve is in position 1. In the passive cycle, the fluid will exit the reservoir because the pump/motor will draw the low pressure fluid through the control valve. The fluid will then enter the pump/motor which will apply a pressure to the system, arrive at the proportional valve where a pressure drop will occur, and then it will pass through the fluid conditioning loop before returning to tank. This process will continue to repeat itself during the passive cycle. In the active cycle, the fluid will again be drawn from the reservoir, but because the control valve will be switched, will be directed through the electrically powered pump which will apply a pressure to it. This fluid will then arrive at the pump/motor powered by the test engine with a higher pressure than that in the passive cycle, thus making the main pump/motor do less work, which will simulate a regenerative braking cycle. Next, it will arrive at the proportional valve where a pressure drop will occur, and then it will pass through the fluid conditioning loop before returning to tank. The two pressure relief valves are in the system as a safety precaution and the heat exchanger assures a correct operating temperature.

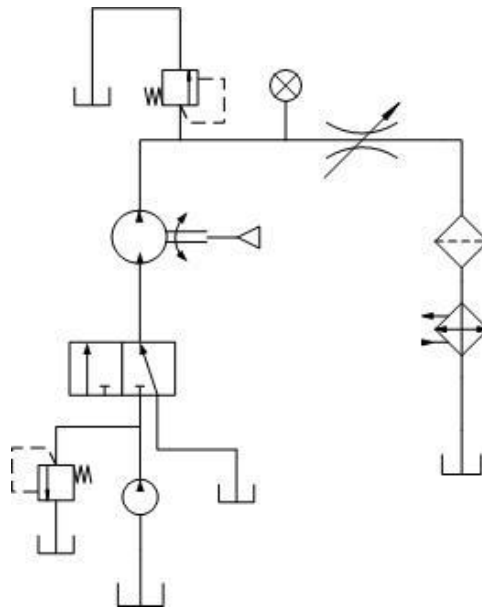


Figure 16: Hydraulic Circuit, Revision G

Individual Component Selection

The hydraulic components within the dynamometer all work together to accomplish the goals of the project, therefore the selection of each individual component is important to achieve the desired outcome. Several issues were driving factors in the selection process including, designing to meet the task specifications, cooling the oil, preventing cavitation and ensuring safe operation of the system. The following section describes the selection process.

Pumps and Motors

The first component to be selected was the main hydraulic pump/motor attached to the machine under test (MUT). The pump/motor had to conform to the task specifications, specifically that it had to exert 20 N•m of torque on the MUT and had to run continuously from 0-3800 rpm. The two basic equations used to determine these factors were

$$T = (p * d) / 2\pi$$

$$Q = d * \omega / 2\pi$$

Where T is the torque, p is the pressure difference, d is the displacement (in in³/rev) ω is the angular velocity and Q is the flow.

A few assumptions were made in order to have a rough idea of an appropriate displacement for the pump/motor. First, it was assumed that the pump/motor would run at 3000 psi at the max speed of 3800 rpm. This resulted in an ideal displacement of 0.371 in³/rev and a maximum flow of about 6.1 GPM. The detailed calculation can be found in Appendix A. Using this as a starting point, pumps with displacements of approximately 0.375 in³/rev were examined. The main pump/motor will have high pressure at both the inlet and outlet ports when run in its different cycles, but many hydraulic pumps could not withstand the high pressures at the inlet ports, so hydraulic motors became the main focus of the search.

A Parker hydraulic motor was found that had a displacement of 0.45 in³/rev with a maximum pressure rating of 2500 psi. This deviated slightly from the ideal conditions, but the increased displacement still allows the pump to run at 20 Nm. The maximum flow of the motor at full speed was found to be about 7.4 GPM and is rated for a maximum of 5000 rpm, which is significantly more than the system's maximum speed.

Once the main motor/pump was selected, the pump powered by the electric motor was selected. The primary concern was maintaining similar flow rates between the two pumps so there was a smooth transition between the active and passive cycles. Applying the same

principles used for selecting the main motor/pump, an ideal displacement was found for the electrically powered pump. The electric motor powering the pump is rated for 1.5 HP and a maximum speed of 1725 rpm. The maximum torque the motor can output was calculated to be 6.2 Nm. The max flow of the main motor was used to find the ideal displacement of the electrically powered pump, which was $0.98 \text{ in}^3/\text{rev}$. A Dynamic gear pump with a displacement of $.82 \text{ in}^3/\text{rev}$ was chosen. This pump produces a flow of about 6.12 GPM, which is close to the flow generated by the main motor. The maximum pressure the pump can produce is 350 psi. Although this is a small pressure increase, it will be sufficient enough to use for academic purposes. If research experiments are being conducted a hydraulic power unit (HPU) can be connected to the system to generate a greater pressure and flow.

Proportional valve

There were few limitations when selecting the proportional valve. The sole purpose of the proportional valve is to dissipate the energy input to the system by the MUT, so overall efficiency of the valve was of little concern. The proportional valve did however need to be rated for a maximum flow greater than the system's maximum flow rate. It was also necessary to control the proportional valve electronically in order to interface with the data acquisition and control system. During the selection process, pressure regulated proportional valves were ignored because the valve needed to apply a variable pressure to the main pump instead of only limiting flow and maintaining constant pressure. Sun Hydraulics' normally open throttle valve (cartridge number FPCH) was selected. This valve operates on 24 VDC with a maximum current of 590 mA. Figure 17 shows the hydraulic schematic of the valve.

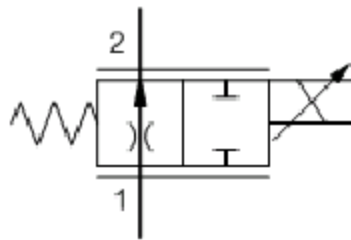


Figure 17: Sun Hydraulics FPCH proportional valve schematic

Control Valve

Unlike the proportional valve, the directional control valve was chosen very carefully to minimize the likelihood of the main pump/motor cavitating. It was necessary that the valve have a pressure drop across it. When in the active cycle, the pressure drop across the valve is

inconsequential because the line is pressurized, therefore eliminating the possibility of cavitation. However, during the passive cycle, the pressure drop across the control valve could lead to cavitation at the inlet of the pump. High flow valves were examined because directional control valves with flow ratings consistent with the system flow rate had very large pressure drops. The valve also had to be electronically controlled so the system could be switched from the active to passive cycle automatically.

Hyvair's D05 high flow valve was selected. The pressure drop across the valve is approximately 5 psi at maximum flow. Figure 18 shows the pressure vs. flow curves for the D05 valve. Note that the curves labeled "T to A" are being used for the passive cycle and "B to A" for the active cycle. The valve is a four port-three position valve, thus, to achieve the design goals, port A was blocked, and only the two right positions were used. Figure 19 shows the original valve schematic and Figure 20 shows the altered valve schematic.

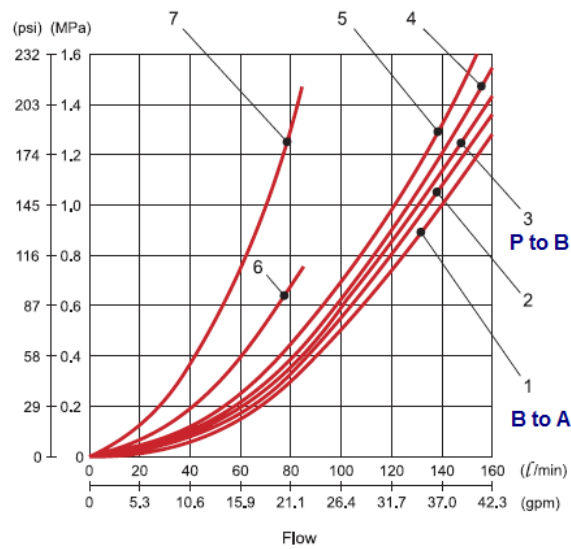


Figure 18: Pressure vs. flow curves for directional control valve



Figure 19: Unmodified control valve schematic

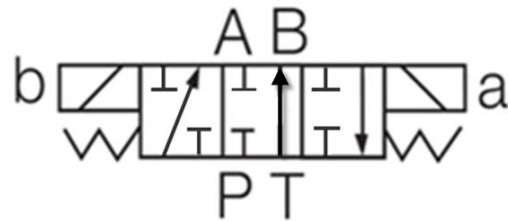


Figure 20: Schematic with "Port B" blocked

Electric Motor

The electric motor was selected to obtain the maximum amount of power a wall outlet can generate. The motor selected runs on either 115 or 220 VAC and draws 15.2 amps at 120 V. This is acceptable for the purpose of the project.

Relief Valves

There are two relief valves placed in the circuit, one after the main pump/motor and one after the electrically powered pump. The relief valves were selected to withstand the maximum system flow of 7.4 GPM. The valves have an adjustable relief pressure and are set so neither of the pumps stall during operation. The relief valve after the main pump/motor is set at 2500 psi and the valve after the electrically powered pump is set at 350 psi.

Filter

The filter was chosen to withstand the systems maximum flow and to provide the proper filtration as specified by the two pumps. It filters out particles greater than 10 microns. The filter was placed at the inlet of the heat exchanger to protect the tubes in the heat exchanger from clogging with debris.

Reservoir

For hydraulic systems it is a good practice to select a reservoir that has a volume at least two times the maximum volumetric flow rate of the system. If there is a heat exchanger in the system, this number can be even lower. Since the maximum flow rate in this system will be 7.4 GPM, the reservoir would have to be approximately 13 gallons. A 15 gallon reservoir was selected due to market availability.

For a hydraulic system to function properly, it is essential that the heat generated by the system be dissipated. Since the system is not doing work, all of the energy produced by the MUT is converted to heat. It was determined that the amount of heat produced by the system was calculated by multiplying the pressure in the system by the flow rate, yielding 8.27kW of heat. The calculations for this design can be seen in Appendix B. These computations were based on a maximum oil temperature of 140° F and an ambient temperature of 95° F.

To determine if a heat exchanger was necessary, the heat dissipation capacity of a 15 gallon reservoir was analyzed. The following conductive and convective resistance equations were used to calculate the overall heat transfer through the walls of a 15 gallon steel reservoir and the surrounding air.

$$R_{conduction} = t_r / K_A A$$

$$R_{convection} = 1 / h_c A$$

$$q_{reservior} = (T_{oil} - T_{air}) / (R_{conduction} + R_{convection})$$

This yielded a result of 214 Watts, proving that an auxiliary heat exchanger was necessary.

Heat exchanger

As previously discussed, there are two common types of heat exchangers: water-cooled and air-cooled. Because the entire application has to be portable it was determined that a tube-finned heat exchanger would be the most suitable for this application. Two methods were utilized to determine the final design. Both methods yielded similar results. The detailed calculations can be found in Appendix C.

Method 1

A tube-finned heat exchanger was found online and the dimensions given were used for the analysis. Heat transfer equations were utilized to find the heat transfer through the fins. The following parameters are dependent on the dimensions of the fins and were used to find their efficiency [1]. It was assumed that the fins were circular, while in reality they were rectangular. The thickness of the fins were assumed to be 1 mm.

$$Parameter_1 = \left(r_o - r_i + \frac{t_f}{2} \right)^{\frac{3}{2}} \left[\frac{2h_c}{K_A t_f (r_o - r_i)} \right]^{1/2}$$

$$Parameter_2 = (r_o + \frac{t_f}{2}) / r_i$$

Where:

R_o is the outer radius of the fin

R_i is the inner radius of the fin

t_f is the thickness of the fin

Using these two values, a graph relating the parameters above with fin efficiency in *Principles of Heat Transfer* [1] was referenced and a value of 93% efficiency was determined. This value (n_{fin}) would be used in the following equation to find the heat transferred by one fin.

$$q_{fin} = n_{fin} h_c 2\pi \left[\left(r_o + \frac{t_f}{2} \right)^2 - r_i^2 \right] (T_s - T_{air})$$

Multiplying this by the number of fins a value of 1.864 kW was obtained. The equations for conductive heat transfer used in the previous section were used to analyze the amount of heat

transferred through the piping where fins were not attached. This resulted in an overall heat dissipation of 2.194 kW. This was not sufficient for the system.

Method 2

Method 2 used more advanced convection techniques to calculate the convective heat transfer coefficient. By splitting the oil cooler into 19 individual pipes the coefficient of convective heat transfer was found. This number determines whether the specified amount of heat can be cooled by normal convection or if forced convection is necessary. If forced convection is necessary, an adequate fan would have to be found to meet the necessary flow rate.

The following equation was used as the starting point.

$$q = mc_p \Delta T$$

The total amount of heat that needed to be dissipated was divided by the number of tubes in the heat exchanger. Using the equation above and algebra the variables were rearranged to solve for the temperature exiting the reservoir ($\Delta T = T_i - T_o$). This value was used to calculate the log mean temperature in the following equation [1]

$$T_{logmean} = (\Delta T_A - \Delta T_B) / \ln\left(\frac{\Delta T_A}{\Delta T_B}\right)$$

Where:

ΔT_A is the temperature difference between the air and oil entering the heat exchanger

ΔT_B is the temperature difference exiting

This was used in the following equation to solve for the convective heat transfer coefficient.

$$h_c = q / AT_{logmean}$$

Where:

A is the total area of all the fins on one tube

Q is the amount of heat needed to be dissipated

$T_{logmean}$ is the logmean temperature found above

The calculated value of 69.671 kg/Ks³ proves that normal convection will be insufficient and forced convection will be necessary. This was reassuring as this value is attainable through the use of a fan. The next step was to determine the velocity that the air would have to move to obtain a proper heat transfer coefficient. The following equation was used and yielded a value of 4.428 m/s [1].

$$U_{max} = \left[\frac{\left(\frac{h_c Pr^{\frac{2}{3}}}{.930 \rho_{air} C p_{air} U_{max}} \right)^{-2}}{L} \right]^v$$

Where:

Pr is the Prandelt number (.71)

v is the kinematic viscosity of air

ρ_{air} is the density of air

Cp_{air} is the specific heat of air

L is the length of the fin

The final step was to find a fan that could provide the necessary velocity in the cross sectional area of the fan hood. A fan blowing 1320 CFM in a hood with the cross section of 14 in. x 16 in. (determined by the size of the heat exchanger) will produce an air speed of 4.311 m/s.

Although the airspeed of the fan is slightly less than what the calculations deem necessary this design will dissipate more heat than the calculation shows. Not taken into account in the analysis was the fact that all the other components (pumps, valves, hoses, etc.) will dissipate heat as well.

Cart

For mobility purposes outlined in the performance specifications, a two-level, steel cart was chosen to attach all the components to. The cart was rated for 800 pounds, limited only by its casters. Since each level is made of 12 gauge steel, deflection was a concern. A load of approximately 400 pounds along with vibrations from the MUT would be applied to the top level of the cart. This level was reinforced with ¼ in x 1 ½ in x 1 ½ in steel angle stock from the underside using metal inert gas (MIG) welds.

Design and Manufacturing of the Components

After all of the system components had been selected and analyzed, the custom design and manufacturing of the rest of the components began. The custom designed and manufactured parts included a cradle to house the main pump/motor, a torque arm, an instrumentation manifold, a mounting plate, and a fan hood. The following sections describe how the parts were designed, manufactured, and integrated into a working system layout on the cart.

Cradle

A dynamometer provides a means for measuring the output torque from a MUT. With a hydraulic system the torque may be calculated using a measured pressure differential across the pump/motor. For this system a different approach was used because of the error created by not having accurate volumetric and mechanical efficiency curves for the pump/motor. The approach for this system was to mount the main pump/motor in bearings and obtain torque through the use of a torque arm. Power is then calculated by multiplying the torque by the angular velocity.

This approach created a need for a means to mount the pump in bearings. Initially, several iterations involved supporting the pump using attachments that housed both the front and back of the pump. This was redirected towards a design which utilized the SAE A 2 bolt mounting dimensions and is referred to as the cradle design. This design can be seen in Figure 21 and the engineering drawings can be found in Appendix D.

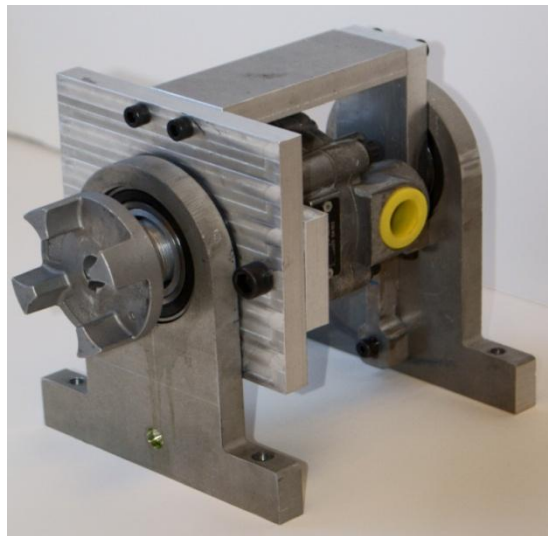


Figure 21: Main Pump/Motor Cradle

The cradle consists of two bearings and six custom-manufactured parts including the bearing mounts, front and back plates, connector block, and torque arm. All custom parts were made from 6061 Aluminum.

The first pump which was selected could not have a high pressure at the inlet, which was necessary for the active cycle. This problem was solved by purchasing a new pump/motor which could handle the system requirements. The new pump/motor had an SAE AA mounting pattern so slight modification to the cradle was necessary. Two fixture tabs were manufactured so that the pump/motor could be properly mounted to the cradle without any further redesign.

Torque Arm

In order to measure the torque of the pump/motor using strain gages, a torque arm was designed to withstand the applied loads and provide sufficient deflection for accurate strain readings. The first iterations of the design had the arm configured horizontally. To conserve space the arm was rotated 90 degrees downward. This allowed for a shoulder screw at one end of the torque arm to prevent rotation.

The strain measurement was taken and torque was calculated using the elastic modulus of 6061 aluminum. The following equations demonstrate the stress-strain relationship to the elastic modulus and the stress in an object subjected to normal bending, respectively:

$$\sigma = E\varepsilon$$

$$\sigma = (M \times c)/I$$

Where M is the bending moment (torque), c is the distance from the outer surface to the center, and I is the moment of inertia of the torque arm. The final designs of the torque arm can be seen in Appendix E and a solid model can be seen in Figure 22.

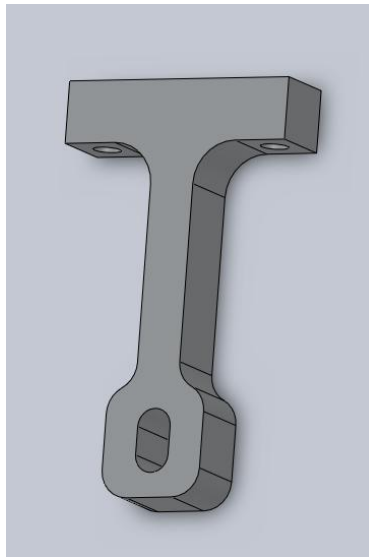


Figure 22: Torque Arm

The dimensions of the torque arm were calculated to optimize the strain readings using the modulus of elasticity and the maximum force output from the MUT. It was modeled as a cantilever beam with a point load at one end. Its thickness was adjusted until the maximum stress in the torque arm was 25% of the yield strength of the material. The MathCAD calculations are available in the Appendix F.

Manifold

A manifold was designed to allow for customization of the hydraulic circuit. Because of the design of the hydraulic system and the limited space of the cart, a conventional hydraulic adaptor could not be utilized. A manifold was designed to bring together the analog pressure gauge and pressure transducer as well as allowing connections for a proportional valve and relief line. The manifold would also act as a sturdy base for these components. The height of the manifold was designed to be the same height as the outlet port of the main pump. This would reduce the lateral forces on the pump from the hydraulic hose. At both ends a #6 SAE port was cut for connections. On top of the block, two ¼” NPT holes were cut for the pressure gauge and transducer as well as a #10 SAE port for the connection of the relief line. All three holes intersected the main through hole. On the bottom of the manifold, two ½-13 UNC tapped holes were added for the mounting to the cart. The manifold was made of 6061 Aluminum for its light weight, low cost and ease of machining. All the machining was done on a manual mill. The engineering drawings are shown in Appendix G.

Manufacturing the Heat Exchanger

There are four main components to the heat exchanger. Two were purchased: the tube-finned oil cooler and the fan, and two were manufactured: the fan hood and legs. The purpose of the fan hood is to force the air to flow over the fins of the oil cooler as well as mount the fan to the rest of the heat exchanger. The fan hood was constructed from an 1/8” thick piece of aluminum that had the hole pattern of the fan cut directly in the middle of it. The sides of the fan were folded up to create a five sided box using a box brake. The fan hood together was welded to ensure there were no gaps for the air to escape as well as adding strength to the structure. Holes were cut on the side to allow for the mounting of legs. 5052 Aluminum was selected as a material because of its ductility for bending.

The legs were designed to be long enough to give the heat exchanger good balance while maintaining a low center of mass. Two holes were cut in the support so it could be mounted to the fan hood as well as two on the feet so that it could be mounted to the cart. 1/8” thick A36 steel was used because its strength and low cost. Because of its strength, the metal had to be heated with an oxyacetylene torch before bending in the brake. The general shape of both the fan hood and the legs were cut in a water jet because milling the shapes from stock would require

a large amount of time and would ultimately waste much of the material. Engineering drawings for the fan hood and stand can be seen in Appendix H, respectively.

Manufacturing the Base Plate

A base plate was designed with multiple mounting patterns in mind. This will make the dynamometer more versatile by being able to easily change the test engine. This includes four through holes to mount the base plate the cart, as well as four through holes for the SAE Baja engine and an array of $\frac{1}{4}$ - 20 threaded holes for other components. The base plate was manufactured out of 6061 Aluminum using CNC machines. The engineering drawings can be found in Appendix I.

System Layout

With all of the circuit components selected, the layout of the system on the cart was designed. There was much iteration in the process, including an attempt to keep everything on a single level as opposed to the two level design that was implemented. In the case of the single level design, there was simply not enough space to fit all of the components and the MUT. The only option in that case was to either mount the MUT, main pump and cradle on two different surfaces, or to remove the main pump and cradle from the cart altogether. It was important to keep all the components and MUT within the confines of the cart to keep the entire dynamometer as functional as possible, so the two level design was chosen.

The main goal in the final cart layout was to minimize pressure losses from the tank to the main pump, provide smooth transition between components to minimize the amount of hose needed, and to allow access to parts that needed either maintenance or adjustment. The first thing to be placed on the cart was the MUT. For simplification, the design was fitted for the SAE Baja engine, a 10 HP Briggs and Stratton Intek engine. However, the cart is still compatible to other test engines.

The first consideration was the need to keep the MUT as far away from the user interface as possible for safety reasons. It was determined that the MUT would be mounted on the top level for easy installation and to allow any test engines to be easily throttled. The MUT fixed the location of the cradle, which is axially in line with the MUT shaft. Both the MUT and the cradle are mounted on a base-plate where they can be moved to suit multiple MUT set-ups.

After the MUT and cradle were fixed, the tank was placed on the cart. The oil level in the tank had to be above the inlet of the pump to keep a pressure head; this meant that the tank also had to be on the top level. With the placement of the MUT and cradle already determined, there was only one appropriate place left to place the reservoir on the cart, as shown in Figure 23. Sufficient space was left on either side of the reservoir for hoses and the placement of other components.

The control valve was the next component to be placed. To minimize the forces applied to the cradle and to allow for the cradle to be repositioned on the cart if necessary, the hose was run from port B through a 90° sweep into the inlet of the main pump/motor. The subplate was also elevated so that the hose running into the pump would be located on the same horizontal plane to minimize the forces on the cradle from the hose; this resulted in more accurate torque readings.

Next, the heat exchanger and electric motor were placed on the bottom layer of the cart. The heat exchanger was placed on the far end of the cart under the MUT to keep the hot air from the heat exchanger and the exhaust from the MUT away from the user. Next, the electrically powered pump was located under the subplate to minimize hose length running from the top of the cart to the bottom. The electric motor was placed where it could fit on the underside of the cart.

The last hydraulic component left to place on the cart was the proportional valve. To save space and keep the hose and fittings as neat as possible, the proportional valve, pressure transducer, and analog pressure gauge were placed in the same manifold. The small profile of all three components allowed the placement of the manifold between the tank and the side of the cart on the top level. This way the user can see the analog pressure gauge to get a basic understanding of how the system is operating from their position at the back of the cart.

Pressure relief valves were added to the system after both pumps. This would insure the pressure in the high pressure regions of the system would not exceed safe operating pressures of 2,500 psi. Both relief valves drained to the reservoir. A return line filter was also added to the system; it was added after the proportional valve and before the heat exchanger. This location was chosen so that if any debris entered the system, it would not plug up the small tubes within the oil cooler. A strainer in the tank also helps protect the system from contamination.

With all the hydraulic components placed, the electronics fit nicely on the bottom of the cart next to the electric motor. The CPU, power supplies and protoboard containing the electrical circuit collecting much of the data were all enclosed in a wooden frame to protect them from leaking oil. Figure 23 to Figure 25 show the cart layout from the top, the bottom level of the cart, and an isometric view of the layout.

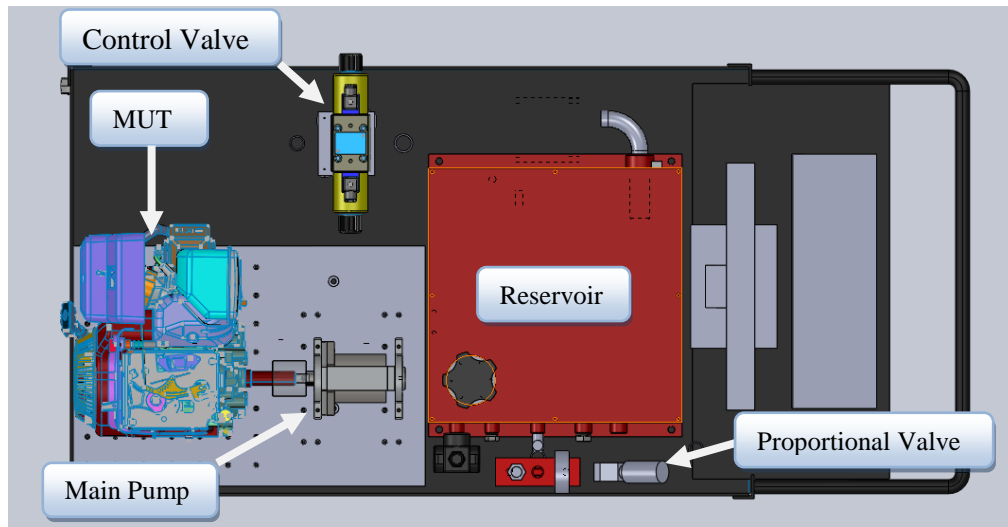


Figure 23: Top level of cart

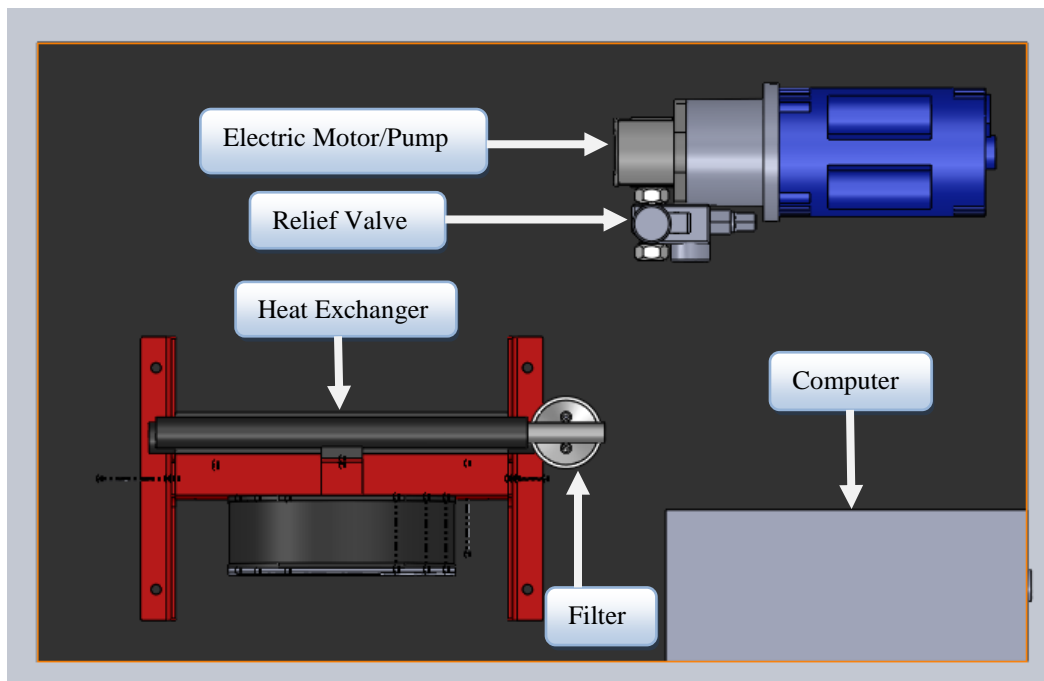


Figure 24: Bottom level of cart

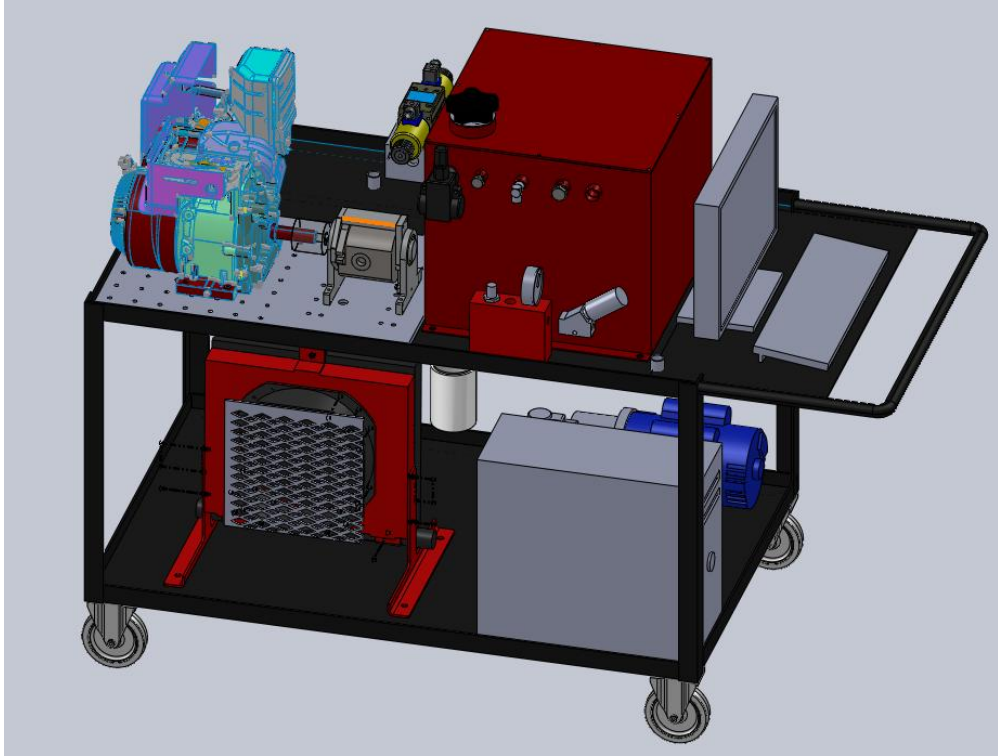


Figure 25: Entire System

Data Acquisition and Controls

One of the goals of the dynamometer was to make it user friendly. In order to do this, acquisition of the experiment data and the control of the experiment had to be automatic and reliable. This encompasses gathering of data from the pressure transducer, torque arm, thermocouple, and angular velocity sensor, as well as controlling experiment parameters such as switching from the active to passive cycle and controlling the torque exerted on the MUT by the proportional valve. LabVIEW was selected as the data acquisition and controls software because of its reputation for being able to accurately measure and control multiple components simultaneously.

Pressure Calculations

For safety reasons as well as determining if the system is working properly, it is necessary for the operator to know how much pressure is in the hydraulic system at all times. A pressure transducer was selected to accomplish this task as well as an analog pressure gauge.

The pressure transducer which was selected measures pressure from 0-3000 psi by generating an output signal of .5V to 4.5V. The voltage received by the DAQ device is related to the measured pressure by applying the equation:

$$y = m * (x - V_{\text{minimum}}) + b$$

where m is the slope, V_{minimum} is in the minimum voltage read, b is the intercept, and y is the calculated pressure. M is calculated for by dividing the pressure range ($3000\text{psi} - 0\text{psi}$) by the voltage range ($4.5V - .5V$). In this experiment, the slope was calculated to be 750 and the V_{minimum} was calculated to be .5V, but after calibration both of these values could change. The intercept value allows the user to calibrate the pressure transducer a bit more precisely, but it can be set to 0 if the user decides that this is the most accurate value.

The analog pressure gauge allows the user to see the pressure in the system which is an added safety feature if the pressure transducer, which requires a DAQ device, fails or is not being read properly. The analog pressure gauge, like the transducer, reads pressure from 0-3000 psi. In both cases, it was possible to select a higher maximum pressure. This was avoided because the system was designed to have a maximum pressure of 3000psi. By having a 3000psi maximum readout for the analog pressure gauge and transducer, the system will be able to record the maximum amount of pressure while also retaining maximum resolution.

Torque

The cradle and torque arm serve an important role in the operation of the dynamometer. The cradle measures the torque exerted by the MUT through the use of the torque arm. By attaching strain gages to the torque arm, LabVIEW can measure strain and relate that to the MUT's torque. A half bridge setup was used to collect the strain data which was fed into an instrumentation amplifier where the signal was amplified before being sent to the data acquisition (DAQ) card. Two equivalent resistors were inserted before the half-bridge to drop the bridge excitation voltage to 10V as specified by the strain gages.

The half bridge set up is ideal for beam bending strain situations. One strain gage is placed on the tension side of the torque arm while the other gage is placed on the compression side of the beam. From the properties of the Wheatstone bridge, the two strain gages work in tandem to double the signal from what only one strain gage could produce. Another advantage of the half bridge is that it will automatically compensate for temperature fluctuations. The resistance of the strain gages is dependent on temperature, but because both gages will be at the same temperature, they will both change by the same amount, cancelling out any change in resistance. The dual strain gage set up also negates the effect of lead wire resistance, which can introduce phantom strain readings.

To compensate for the small unconditioned signal from the strain gages, an instrumentation amplifier was built. The instrumentation amplifier takes the signal from both arms of the bridge and amplifies the difference between the two signals. The output of the instrumentation amplifier is then fed into the DAQ card to be read. The gain for the amplifier is 84.9 and was selected so the range of the output voltage from the amplifier at maximum torque is about 200 mV. This is the smallest range the DAQ card can be set to and gives the highest resolution, approximately 6 μ V. Two capacitors were also inserted between both the plus and minus 12 V power rails and ground to eliminate small fluctuations in the voltage coming from the power supply. While these capacitors do not completely eliminate electrical noise from the circuit, they provide a more stable signal from the power supply. Figure 26 shows the circuit diagram for the instrumentation amplifier.

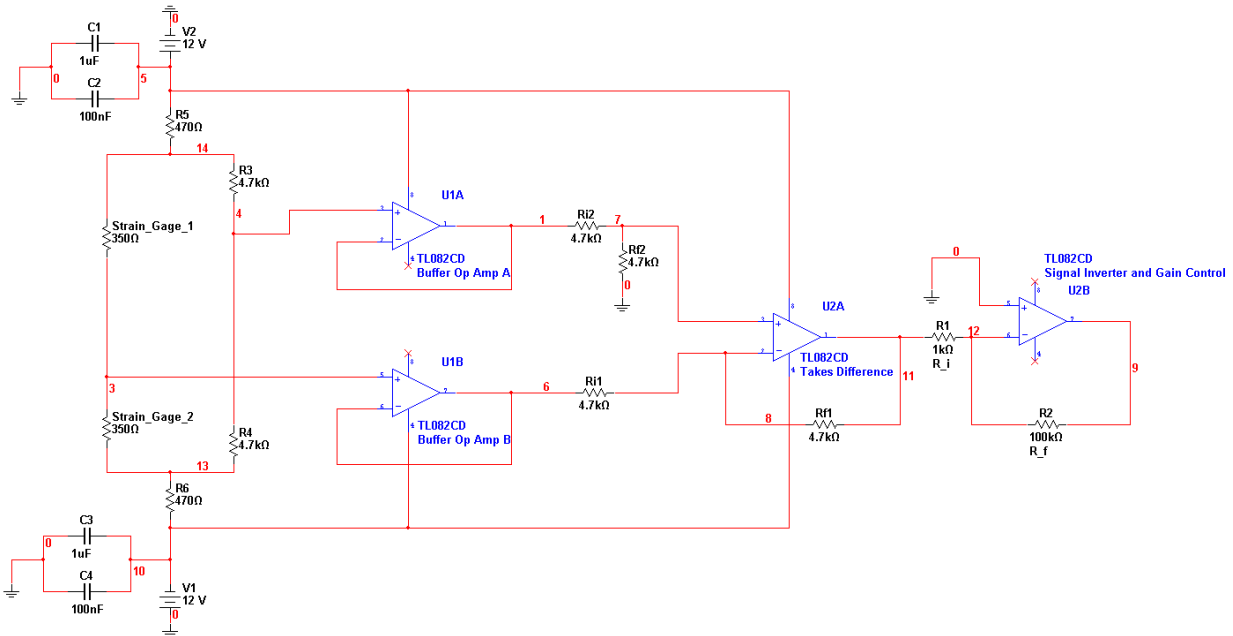


Figure 26: Instrumentation Amplifier

The torque values calculated in the LabVIEW VI are used in a feedback control loop of the proportional valve. As the proportional valve closes, it exerts a torque on the MUT, which is measured by the strain gages. This principle was used in developing a control feedback loop that controls the position of the proportional valve by inputting a user defined torque. First, the user inputs their desired torque. At that time, there is a torque being exerted on the torque arm; that signal is fed back into the user defined input torque and their difference is sent to the proportional, integral, and derivative (PID) controller block in the LabVIEW VI. The controller amplifies the signal and sends it to the proportional valve which adjusts accordingly. The new position of the proportional valve changes the torque being measured by the torque arm, which again negatively feeds back to the PID controller. This process repeats until there is zero error. Figure 27 shows a block diagram representing the controller. The calibration of the PID controller will be discussed in subsequent sections of this report.

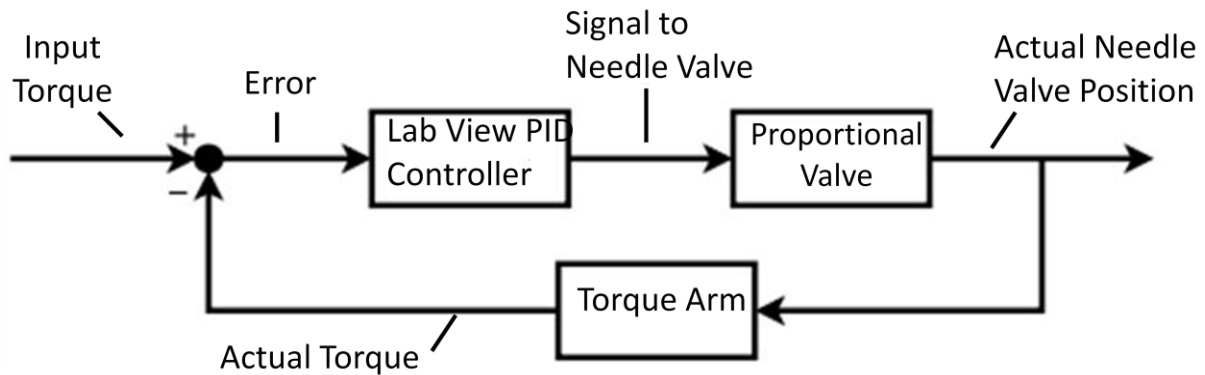


Figure 27: Block diagram representation of proportional valve PID controller

Proportional valve

The control of the proportional valve underwent many different phases until the final pulse width modulation (PWM) design was chosen. The proportional valve is controlled with a solenoid that exerts a force on the pin that restricts the orifice in the manifold of the valve. The position of the pin is determined by the current flowing through the solenoid, which must also be kept at a constant 24 VDC. It was necessary to control the proportional valve with either an analog voltage or current coming from the DAQ card, so purchasing a separate variable current source was not possible.

The first concept was to operate the valve using a variable transistor that would vary the current drawn through it based on a variable input voltage. This concept was discussed with Professor O'Rourke from the Electrical and Computer Engineering (ECE) department at WPI, however, it was soon discarded because it quickly became too complicated and would require too much time to develop.

After the variable transistor design was no longer an option, the idea of using pulse width modulation to control the valve was entertained. PWM works by pulsing a constant signal voltage at high frequency on and off, generating a square wave. The duty cycle of the PWM signal is defined as the percent of time that the signal is on. Figure 28 shows an example of different duty cycles for a PWM signal.

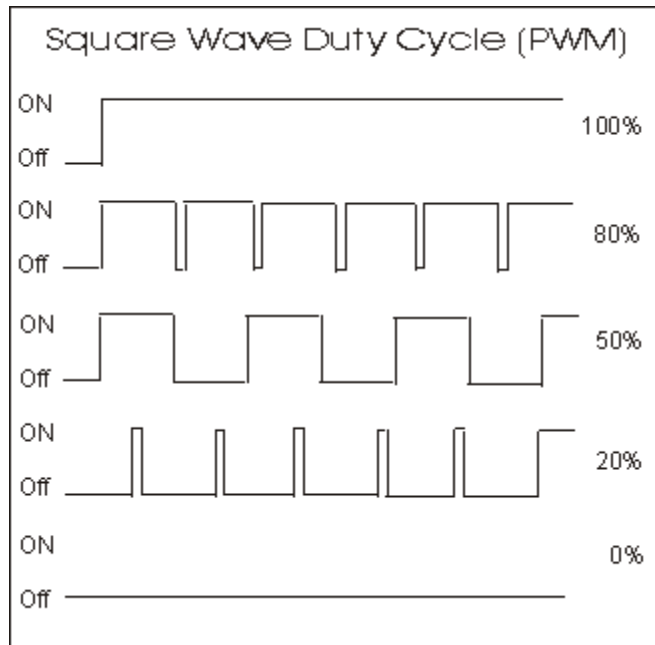


Figure 28: PWM duty cycles

Texas Instruments' DRV 101 pulse width modulation circuit was the first to be tested. The DRV 101 is an internal circuit (IC) that creates a fixed 24 kHz frequency PWM signal whose duty cycle is adjusted from 10-90% by a variable voltage. This solution seemed to fit the criteria, however, when testing the proportional valve with this IC, the valve would not move. Most likely, the frequency of the IC was too high to be able to switch the amount of current being drawn by the solenoid through the IC. The next step was to build a custom PWM circuit with a lower frequency.

The new PWM circuit was built following Professor O'Rourke's Multisim model for a PWM circuit operating on a single source voltage supply. The output of the circuit is a PWM signal at 138 Hz. The duty cycle is adjusted by varying a voltage to one of the inputs of the op-amps. The voltage range for the duty cycle varies from about 7 to 18 volts, but the analog output of the DAQ card can only output 0-10 volts. To overcome this obstacle, a separate op-amp was built into the circuit that doubles the output of the DAQ card giving the circuit an effective range of 0-20 volts. A circuit diagram of the PWM circuit is shown in Figure 29.

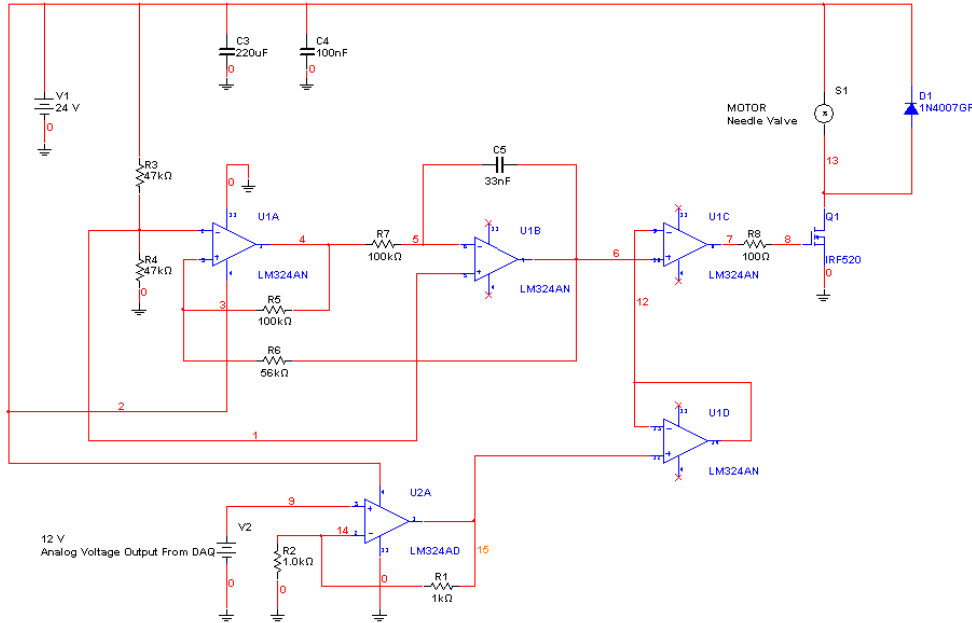


Figure 29: PWM Circuit

Directional Control Valve and Electric Motor

The electric motor and directional control valve both are involved when switching between the active and passive cycle. To control their operation, relays were used to switch them on and off. In both cases, a digital output is sent from the DAQ to the reed side of the relay. When the reed closes, the circuit is completed and the valve switches or the electric motor turns on.

Angular Velocity

One of the main pieces of data which the system needs to compute is power, which is calculated by multiplying the torque by the angular velocity. Therefore, the angular velocity must be recorded by some means and it was decided that the use of a magnetic Hall effect sensor was the most appropriate.

The Hall effect sensor was mounted to an L- bracket on the front bearing mount. The position of the sensor in relation to the magnet is critical for proper data acquisition. With each rotation of the shaft, the Hall effect sensor it generates a spike in the signal caused by the magnet. Each spike is counted and the total is divided by the time between each rotation to give an output of angular velocity in revolutions per minute.

The magnet is fixed to the shaft by a slot milled in the Lovejoy coupler between the main pump/motor and the MUT. A set screw hole was drilled perpendicular to the slot to secure the magnet in place. This placement allows the Hall effect sensor to consistently register with each rotation.

Experiment Set Up

In order to properly obtain and record all of the desired results it was necessary to develop an experiment using a data acquisition device. An experiment allows a user to customize what data is received from the system (data acquisition) as well as what signals are sent to the system (controls). The experiment which was developed is unique to the goal of this project and while individual components within the experiment could be used for other applications, the experiment as a whole was developed for the sole use in this project. It was determined that LabVIEW, a product developed by National Instruments, would be the software which was used to create this experiment.

LabVIEW is a data acquisition and control software which allows a user to have nearly full customization over the system which they are observing. The software is a graphical programming language which results in a user friendly interface which is beneficial to those who are not experienced with programming languages. Further, LabVIEW has an extensive library of tools which allow the user to develop the entire program using one single software.

The experiment developed incorporates many different components, most of which need to record or generate values at extremely fast and precise rates. Because of this, it was desired that the program runs as efficiently as possible. This resulted in a stacked sequence structure being incorporated into the program so that the program completes tasks as the user desires. The first step is to establish all of the channels and input all of the preliminary conditions. Next, the inputs and outputs are read or generated and calculations are completed. Finally, the data is recorded to a spreadsheet so that the user can analyze the tests completed at a later time.

Selection of DAQ Device

The correct selection of the DAQ device was critical to the successful completion of this project. If an improper DAQ card was chosen it would not have the sufficient input and output channels required for the components which were selected. Because of this, it was necessary to determine all of the components which would generate signals or needed to be controlled and establish what types of channels were necessary for these components to work properly. Table 3 outlines the components and necessary channels.

Table 3: Components and Channels Necessary

Device	Channel Type
Pressure Transducer	Analog Input – Voltage
Electric Motor	Digital Output
Control Valve	Digital Output
Proportional valve	Analog Output – Voltage
Strain gage	Analog Input – Voltage
Hall effect Sensor	Digital Input/Counter
Thermocouple	Analog Input - Voltags

Once all of the channels required have been determined, a proper DAQ device could be selected. National Instruments was the company which was used to purchase all of the necessary components because of their great reputation and their relationship with WPI which resulted in a 10% discount. It was determined that the NI PCI-622X series would be adequate. Because the proportional valve requires an analog output, many boards were no longer sufficient for this project. The NI PCI-6221 was determined to be the best fit because it had all of the necessary inputs and outputs and the price was within the operating budget. Table 4 outlines the specifications for the NI PCI-6221 DAQ card which was purchased.

Table 4: Channel Types and Amount on NI PCI-6221

Channel Type	Number of Slots
Digital I/O	24
Analog Input	16
Analog Output	2
Counters	2

A connector block (CB-68LP) and a cable (1 meter SHC68-68-EPM) to connect the DAQ card to the connector block were also purchased through National Instruments.

Individual Components

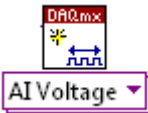
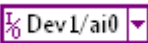
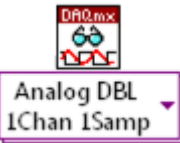

The creation of virtual channels as well as calculations for many of the components was required for the system work properly. The following describes how each of these components was added into the experiment.

Pressure Transducer

The pressure transducer was set up as an analog voltage input. As discussed previously, the DAQ receives a voltage signal that varies between .5 and 4.5 volts and corresponds to the amount of pressure in the system. The voltage is inserted as the x value in the equation

$y = m * (x - V_{minimum})$, where m is the slope, $V_{minimum}$ is in the minimum voltage read and y is the calculated pressure. In this experiment, the slope was calculated to be 750 and the $V_{minimum}$ was calculated to be .5V, but after calibration both of these values could change. Depending on the testing circumstances (heat, type of oil, etc.) it might be necessary and useful for the user to again calibrate the pressure transducer to assure that it is recording the proper value. The creation of a virtual channel for the pressure transducer can be seen in Figure 30, while the calculations for the $y = m * (x - V_{minimum}) + b$ equation can be seen in Figure 31. Table 5 outlines how the reader can interpret most of the LabVIEW block diagrams.

Table 5: How to Interpret LabVIEW Block Diagram

Component	Function
	This device establishes the type of signal which LabVIEW will be reading. In this case, the signal is an Analog Input of Voltage.
	This determines the channel which the signal will be read from. This component depicts Device 1, Analog Input 0.
	This device designates that the data will be read by LabVIEW and establishes the method to do this. In this case it is reading one sample from the channel, it can also be set to read multiple samples from the same channel.
	This is determining that LabVIEW will output a value to another component. The signal can either be digital or analog, but in this case, it is generating a digital (on/off) signal.

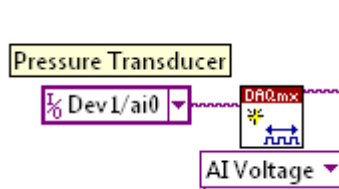


Figure 30: Creation of Virtual Channel for Pressure Transducer

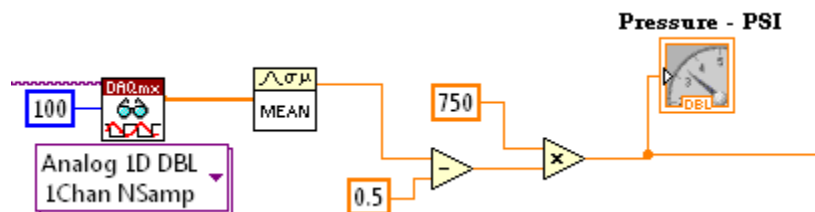


Figure 31: Calculations for Pressure Transducer

Electric Motor

The electric motor is set up as a digital output. A digital output allows the user to have the system in either an on or off position and generates a voltage of either 0 volts (off position) or 5 volts (on position). The control of this on or off switch is on the front panel and switches the system between the active and passive cycle. The electric motor is only on during the active cycle, and thus, if the user is running the system in the passive cycle the electric motor is not turned on. However, in the active cycle the +5V is generated by the DAQ device which turns on the motor. Figure 32 shows the creation of the virtual channel while Figure 33 shows how the DAQ device generates the signal.

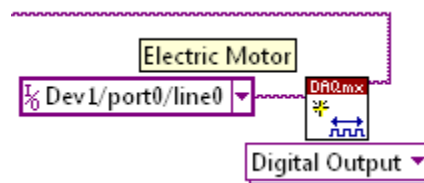


Figure 32: Creation of Virtual Channel for Electric Motor

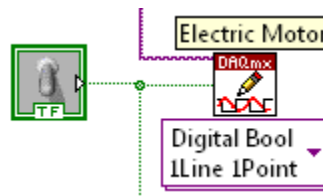


Figure 33: Generation of the Signal for the Electric Motor

Control Valve

The control valve, like the electric motor is a digital output. It is necessary for the control valve to be in two different positions, one which is used in the active cycle and the other which is used in the passive cycle. The position in the passive cycle is the neutral position of the valve, and therefore no signal needs to be sent to the valve. In the active cycle however, a signal needs to be sent to the valve to change its position. Through a relay switch, the 5V signal generated by the DAQ device switches the control valve between its neutral position and the desired position. The creation of the virtual channel for the control valve can be seen in Figure 34 and Figure 35 shows how the DAQ device generates the desired signal.

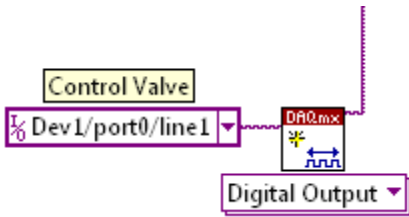


Figure 34: Creation of Virtual Channel for Control Valve

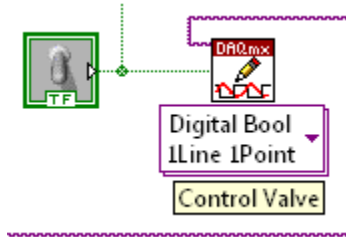


Figure 35: Generation of the Signal for the Control Valve

Proportional valve

The proportional valve is the sole analog voltage output in the system. As described in a previous section, the position of the proportional valve varies dependent upon a variable voltage. The analog voltage output generates a signal between 0 and 10 volts, but for safety reasons the maximum and minimum output voltages are 8.5 and 3 respectively. One of the task specifications for the project was for the user to have the capabilities of specifying the torque on the MUT. This was accomplished by the control feedback loop which automatically adjusts the proportional valve's position. In order to do this, a PID controller, as discussed above, was used and the voltage generated by the DAQ card was in direct relation to this loop. The PID control loop can be seen in a subsequent portion of this report. The creation of a virtual channel for the proportional valve can be seen in Figure 36 and the signal being generated can be seen in Figure 37.

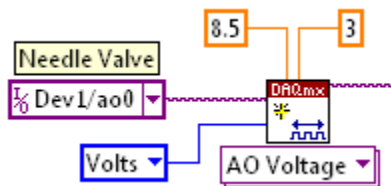


Figure 36: Creation of Virtual Channel for the Proportional valve

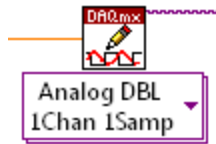


Figure 37: Generation of the Signal for the Proportional valve

Strain Gage

In order to properly determine the power of the system the torque needs to be determined. The strain gage instrumentation amplifier circuit generates a voltage which is read by an analog voltage input channel that is created in the experiment. The channel and its reading can be seen in Figure 38 and Figure 39 respectively. The calibration of the strain gage will be discussed in subsequent parts of this report.

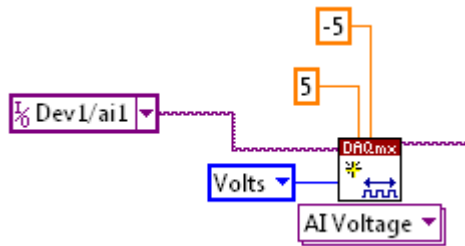


Figure 38: Creation of Virtual Channel for the Strain gage

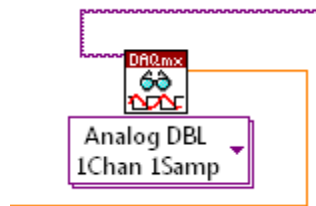


Figure 39: Computing the Strain gage Signal

Hall Effect Sensor

The DAQ device which was purchased has a counter channel. A counter channel records the number of occurrences and divides it by the time, resulting in frequency. This is ideal for this circumstance and returns the frequency of the MUT's shaft. Figure 40 shows the creation of the counter channel while Figure 41 shows how the experiment reads the data.

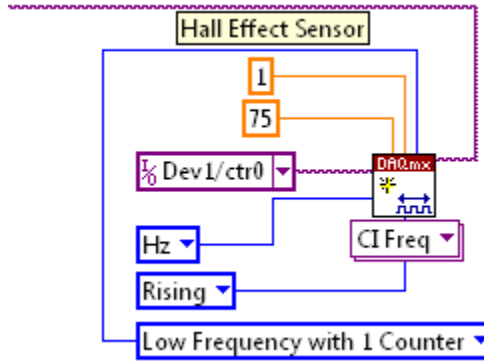


Figure 40: Creation of the Virtual Channel for the Hall Effect Sensor

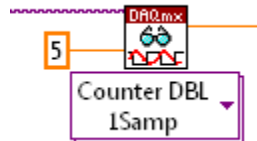


Figure 41: Reading the Data of the Hall Effect Sensor

Calculations within Experiment

With all of the components having their signals properly recorded or generated, additional calculations are required to integrate the system.

Power Calculation

The calculation of the power of the MUT, as stated before, was a task specification of this project. In order to do this, the calculated torque needed to be multiplied by the angular velocity. A formula node was created in the experiment to compute this calculation simultaneously with the acquisition of the data. Having this process completed simultaneously with the generation and recording of signals is beneficial because it allows the user to see exactly how the power changes as the torque input is changed. The formula node can be seen in Figure 42.

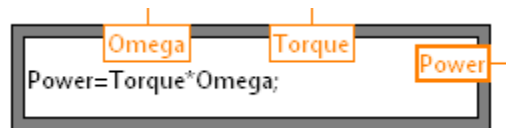


Figure 42: Formula Node for Power Calculation

PID Controller

The PID controller allows the user to set a desired torque and have the proportional valve automatically change based on the operators input. By having the PID controller internal to the

LabVIEW VI, computing power is saved. The user sets a desired torque and this is compared to the actual torque on the MUT. Using a graph to compare these two values the user is able to tune the PID controller and determine the appropriate gains. Figure 43 shows the PID feedback loop.

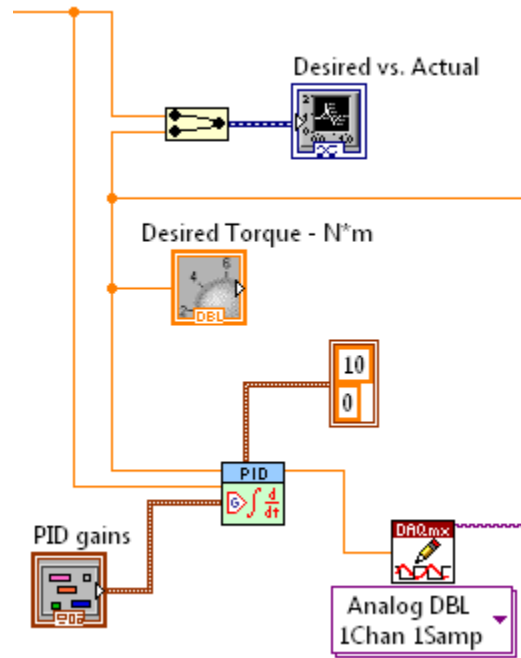


Figure 43: PID Controller Feedback Loop

Active and Passive Cycle

As it was alluded to in a previous section, only two components need to be controlled to switch between the active and passive cycles: the electric motor and the control valve. Although the proportional valve will also change position, its position can change at any time, not just in the active cycle. The user will have a switch on the Front Panel which can be seen in Figure 44 that toggles the system between the active and passive cycle.

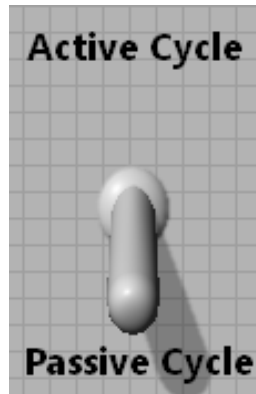


Figure 44: User Control to Switch Between Active and Passive Cycles

The switch being toggled results in two changes occurring. The electric motor is turned on and the control valve is switched. Figure 45 shows the programming for this aspect of the system.

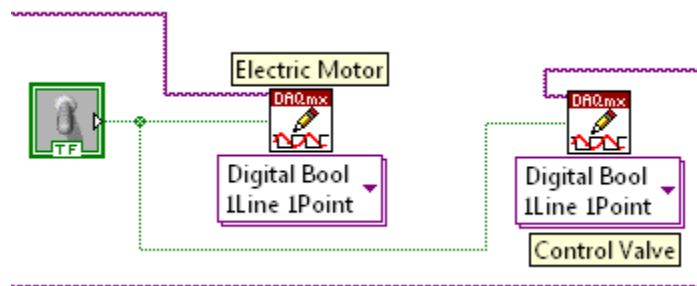


Figure 45: Active and Passive Cycle Loop

By controlling the electric motor and control valve with one switch, the system will simultaneously change the control valve and turn the electric motor on. This is important because otherwise there could be the possibility of cavitation, or stalling the electric motor.

Recording the Data

Once all of the data is gathered the user will be able to record it to a spreadsheet. On the front panel the user will have the option of whether or not to record the data and where to record the data. If the user decides to record the data, a Microsoft Excel spreadsheet will be generated that includes the recorded power, torque, angular velocity, pressure, and temperature during the experiment as well as the time history.

Benefits of the Experiment

This experiment has many benefits which will allow the user to customize the experiment to achieve their desired results. All of the values can be calibrated and changed so that if

different components are substituted, the whole experiment does not need to be changed; only coefficients need to be adjusted. The experiment was also developed to have an advanced interface or a basic interface. If the basic interface is chosen the user only has two controls, the switching between the active and passive cycle, and the input torque. If the system is run in the advanced interface, the user will have full ability to easily adjust all experiment parameters.

User Interface

The user interface is an important part to the DAQ system because even if all of the data is recorded properly and the components are controlled, the user needs to be able to easily use the system. As stated above, two models were developed, a basic interface and an advanced interface. Figure 46 depicts the basic interface while Figure 47 depicts the advanced interface.

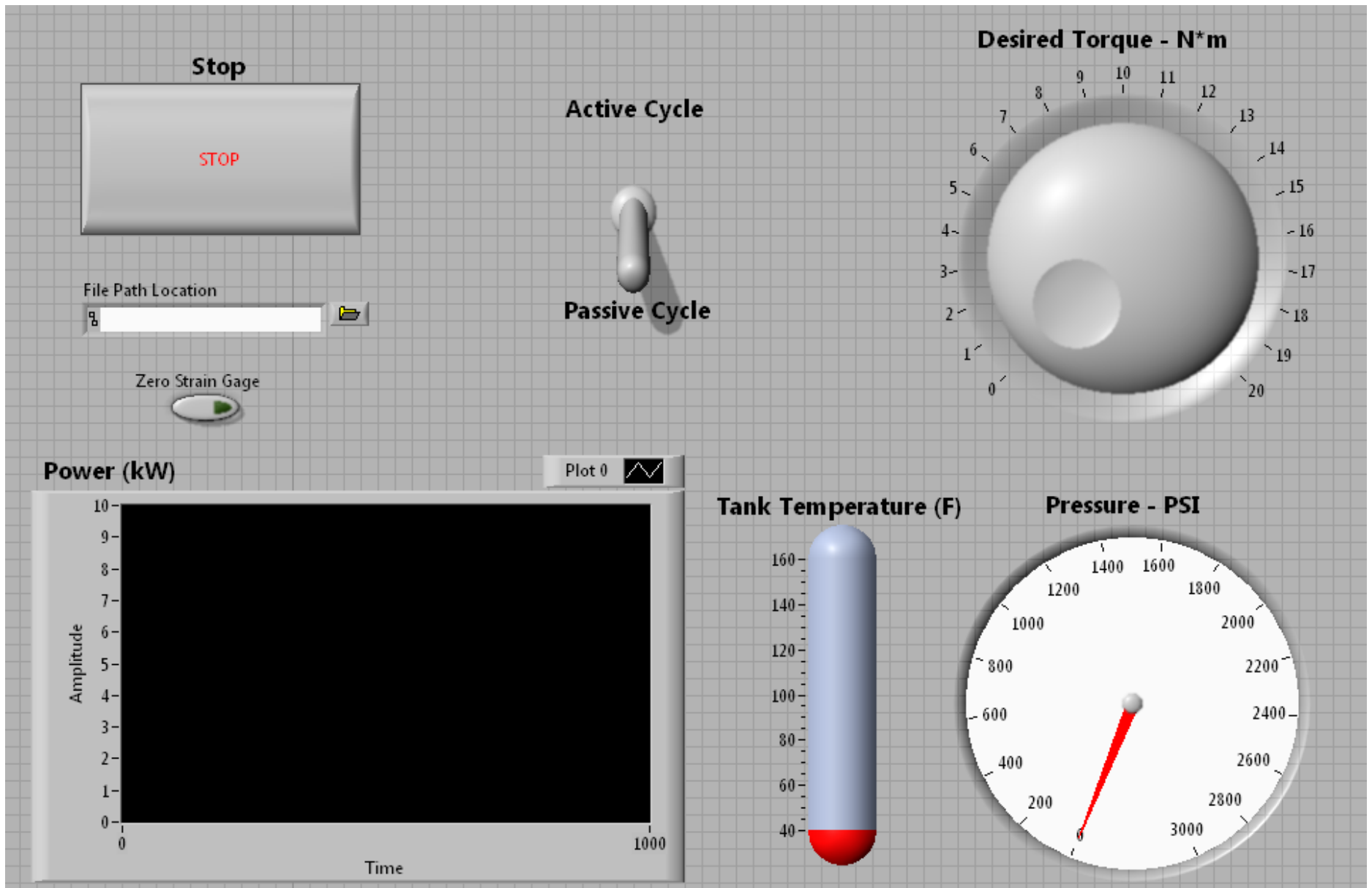


Figure 46: User Interface - Basic

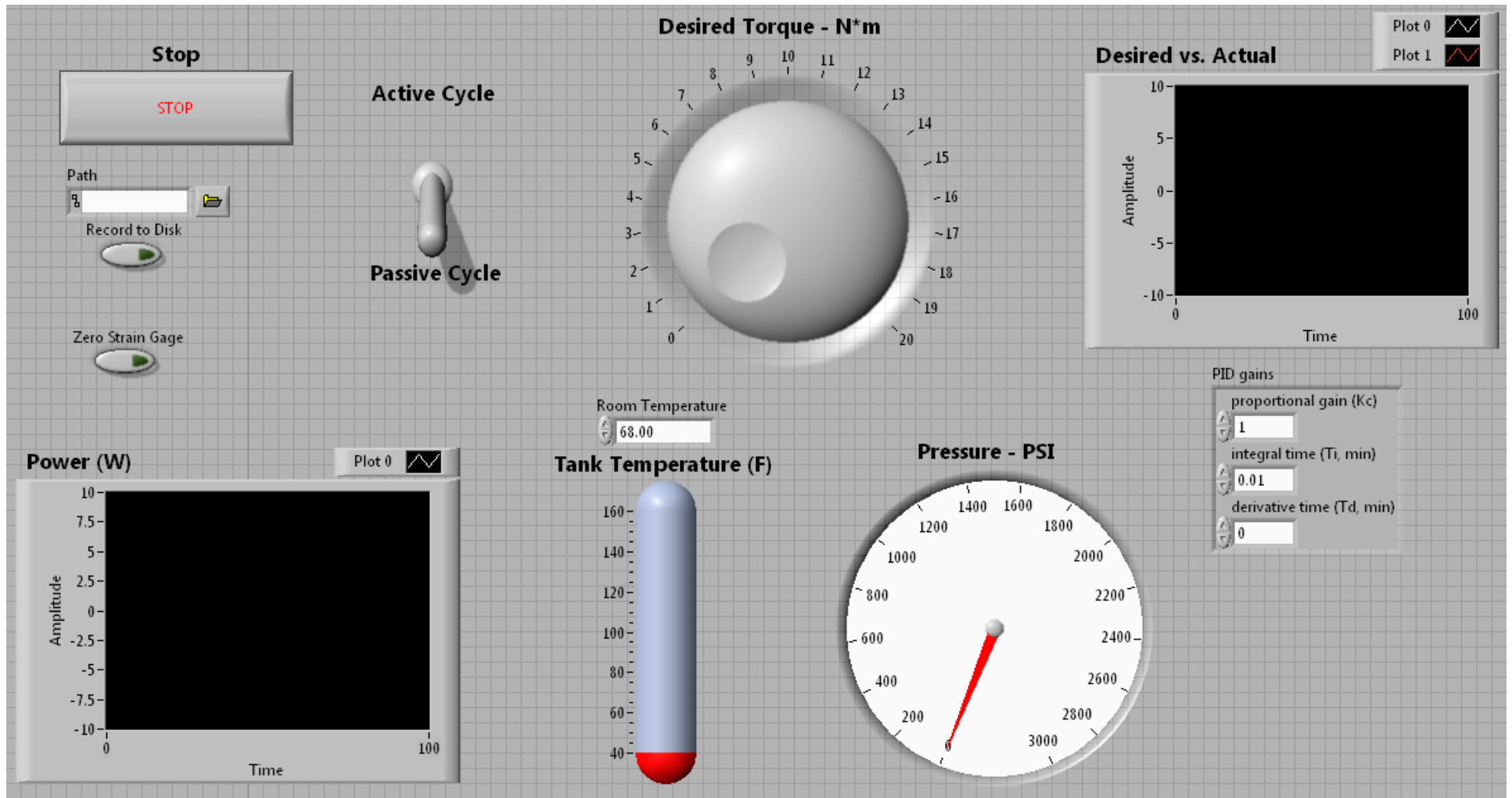


Figure 47: User Interface - Advanced

Final Testing

The objective of this project was to develop a hydraulic dynamometer which simulates the regenerative braking cycle. In order to accomplish this goal, final testing was conducted to assure the dynamometer was working properly.

Calibration

To determine if the system was working properly, it was necessary to calibrate the system to assure that accurate test data was being received. To determine the performance of the MUT, the angular velocity is multiplied by the torque. The angular velocity, because of how it was established in the experiment does not need to be calibrated because the experiment is simply counting how many times the magnet passes the sensor and then dividing it by time. The torque measurements however, needed to be calibrated to assure proper readings. Additionally, the PID controller needed to be calibrated so that the proper values for the P, I, and D gains were determined.

Strain Gage

In order to calibrate the strain gage, a series of tests were done prior to running the system. A strain gage varies resistance with strain and, when configured in a bridge, outputs a voltage which relates to the amount of strain. This voltage can be related to the torque about the shaft through a series of equations involving the geometry and material properties (Method 1), or can be directly related to the torque through calibration (Method 2); both of these methods were attempted. Further, a gain of 84.9 was added through an instrumentation amplifier to amplify the voltage signal produced by the strain gages and result in more accurate readings.

In order to calibrate the system, a known force was applied to the main pump/motor at a known distance, allowing the torque to be calculated. To conduct this calibration process, a spring scale was used which could output values between 0 and 10kg. Values of 2, 4, 6, 8 and 10kgs were all tested and applied at a distance of about .05m. With the expected force being able to be calculated ($Torque = Mass * g * distance$), the values recorded could be recorded and the error could be determined.

Each of the masses was applied 4 separate times, the relationships were averaged, and error was determined. It was also determined after multiple tests that a mass of 2kg was an outlier, so this value was excluded from the averages. This is most likely attributed to the

friction in the torque arm absorbing most of the force instead of the torque arm itself. It should be noted that the equipment available only allowed for a maximum torque of 4.9 N•m to be calibrated for, so there could be some possible error. All of the test data for both methods can be seen in Appendix J.

Method 1

A series of equations were used to relate the measured voltage to a torque and then the final result was multiplied by some constant; this constant was the calibration factor. The equations which were used can be seen below:

$$\frac{2 * V_{measured}}{F * V_{initial}} = Strain$$

$$\frac{Strain * I * E}{c} = Moment$$

$$\frac{Moment * r_1}{r_2} = Torque$$

The *Strain* equation takes the measured voltage output from the strain gage and relates that value to strain. The *Moment* equation relates the strain to a moment, and the *Torque* equation relates the moment to a torque about the shaft. It was determined that the approximate relationship was 3.12 with an average error of less than 1.2%.

Method 2

Method 2 eliminated the equations and directly related voltage to torque. The measured value of voltage was multiplied by a constant, which was the determined relationship between the voltage output and the corresponding torque. It was determined that a relationship of 56.549 existed between the voltage and actual torque, with an average error of 2.5%.

Comparing Method 1 and Method 2 led to the determination of which system would be used in the system. Method 2, although not as accurate was still within an acceptable level, and also required less computing power within the experiment because the measured value is only being multiplied by one constant, instead of nearly a dozen. The difference in accuracy between Method 1 and Method 2 can most likely be attributed to user error. The calibration tests were performed by plotting the output signal on a chart and taking the average of the output. This

average was taken by eye, because no better method was known, and therefore the difference in error can most likely be attributed to user error.

Although the calibration led to an accurate result in the lab, the data contained a great deal of noise when the diesel engine was actually turned on. The engine had a great deal of vibration which really disrupted the strain gage measurements and resulted of torques from 2 N•m to 8 N•m being calculated with no load applied to the system. In order to lessen this error a 2 pull low pass filter was used in labVIEW. This filter had a cut off frequency of 1Hz which will filter out all electrical noise as well as the vibrations from the test engine.

PID Controller

Due to unforeseen complications during calibration, the PID controller was not tuned at the time of publication. If final values of the PID controller would like to be seen, please contact Professor James D. Van de Ven to obtain the User's Manual for the Hydraulic Dynamometer.

Remaining Components

Each of the other components were tested and it was determined that they were working properly. The thermocouple and pressure transducer were not critical components to data being tested and thus, calibration was not crucial. Both the thermocouple and pressure transducer were recording values within 5% of the value determined by the thermometer and pressure gauge respectively.

Results

The performance of the MUT was determined using the data acquisition system. Figure 48 shows an example of a power curve for the MUT. The first plot shown, labeled waveform chart, is the plot of angular velocity in RPM, the second chart, labeled torque, is the torque readings for the MUT with respect to time, and the final plot is the power output. It should be noted that an omission was made in the final calculations of the power. The angular velocity needs to be in rad/s but was left in rpm. When this conversion factor of approximately 0.10471 was applied to the data, the maximum power generated was approximately 5HP, instead of 50 as depicted in Figure 48. The actual power output of the test engine is unknown, and thus, the calculated data cannot be compared. This is, however, the same range which was expected and the calibration process led to appropriate values of torque. Combined with the fact that it is a ten horsepower engine and the throttle was half way open leads us to believe the results are accurate.

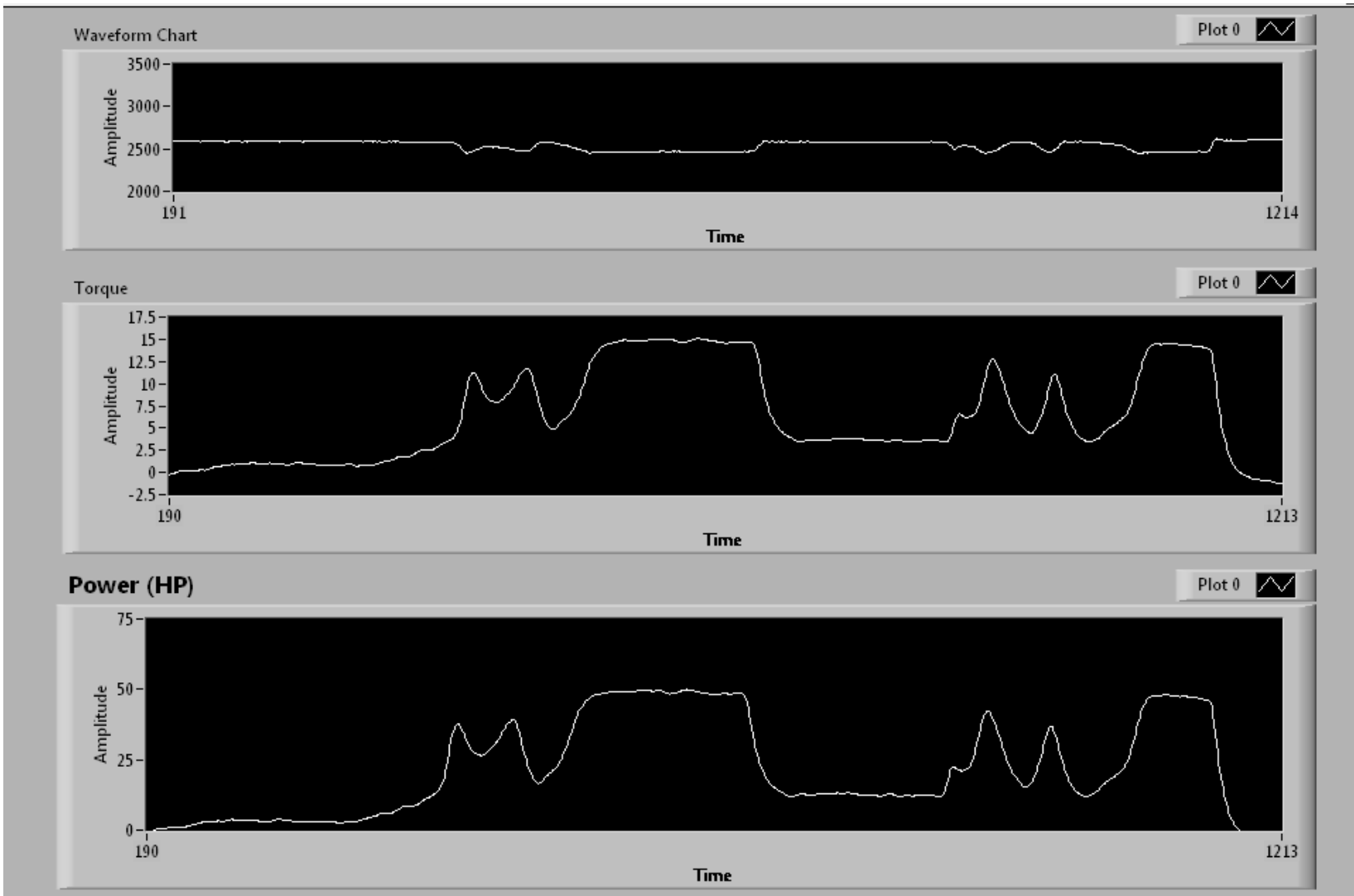


Figure 48: Results for Diesel Engine

Data was recorded to a spreadsheet in a subsequent test and was manipulated to take into account the conversion factor between rad/s and rpm. This data can be seen in Figure 49.

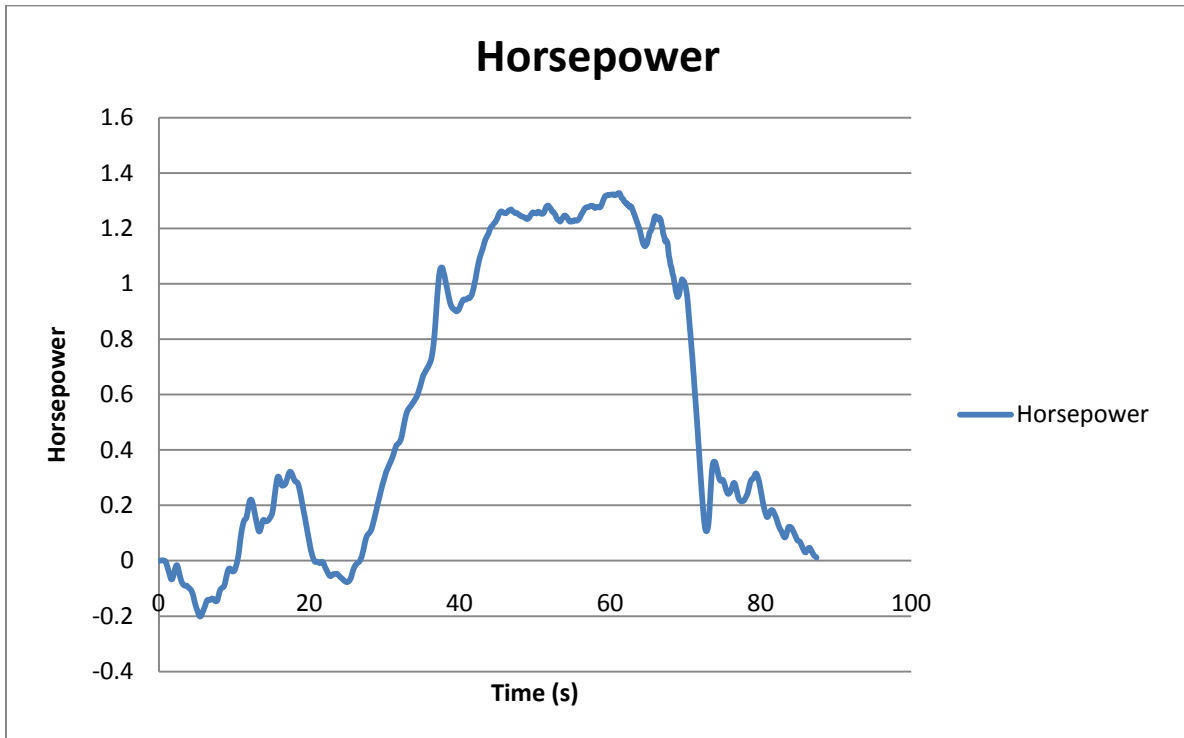


Figure 49: Horsepower of MUT

This test had a maximum pressure of only 500psi, 20% of the potential, leading to the smaller power readings. The results include a negative power output because at that point in time the strain gages were measuring a negative torque because of signal noise. This can be addressed with subsequent data manipulation. The remainder of the results can be seen in Appendix K.

At the time of publication, errors were being encountered when all components of the experiment were being executed simultaneously. Thus, the program was not able to record data for the torque, angular velocity, pressure, and temperature while also controlling the proportional valve, and active/passive cycle. To obtain a complete working copy of the .VI, please contact Professor James D. Van de Ven to obtain the user's manual for the hydraulic dynamometer.

Future Recommendations

After completing the project, the following recommendations can be used to improve the performance and accuracy of the system.

Load Cell

It is recommended that a load cell replace the torque arm and strain gage assembly. This would house and protect the strain measurement device. This would also provide more accurate results that were caused by exposed strain gages and wiring.

Variable Displacement Pump for Electric Motor

It is recommended that the fixed displacement pump powered by the electric motor be replaced with a variable displacement pump. Currently, the flow rate of the electrically powered pump matches that of the main pump/motor when the MUT is at maximum power. Therefore, the electrically powered pump will only work if the MUT is at full throttle or 3600 rpm. By utilizing a variable displacement pump powered by the electric motor, the flow rates would be able to be matched at various throttling speeds.

Dampening Vibrations

To decrease the vibrations throughout the cart and to reduce noise in the measurements of strain, it is recommended that actions be taken to dampen the vibrations from the MUT. One possible solution is to place a vibration dampening material between the MUT and the cart. Another solution is to add a hydraulic or pneumatic dampener to the system. Further, a flywheel could be placed on the shaft of the main pump/motor to absorb the natural harmonics of the MUT. This will help to eliminate noise in the measurements of torque through the strain gages.

References

- [1] Bohn, Mark S., Krieth, Frank. *Principles of Heat Transfer*. -6th ed. Brooks/Cole, 2001.
- [2] Cundiff, John S. *Fluid Power Circuits and Controls*. N.p.: CRC Press, 2002. Print. Mechanical Engineering Ser.
- [3] Eaton, *Industrial Hydraulics Manual*. 2008. Print. Eaton Fluid Power Training.
- [4] Lampton, Christopher. "How Regenerative Braking Works." *How Stuff Works*. Discovery, 2009. Web. 14 Oct. 2009. <<http://auto.howstuffworks.com/auto-parts/brakes/brake-types/regenerative-braking4.htm>>.
- [5] *Powered by Dyamometers*. N.p., n.d. Web. 14 Oct. 2009. <<http://www.powerdynamometers.com/types-of-dynamometers.php>>.

Appendix A: Sizing of Hydraulic Pump

Maximum Torque	$T := 20 \text{ N}\cdot\text{r}$		$\text{psi} := \frac{\text{lbf}}{\text{in}^2}$
Pressure	$p := 2500 \text{ psi}$		
Angular Velocity	$\omega := 3800 \frac{\text{rev}}{\text{min}}$		$\text{GPM} := \frac{\text{gal}}{\text{min}}$
Displacement	$d := \frac{T \cdot 2 \cdot \pi}{p}$	$d = 7.29 \text{ cm}^3$	$d = 0.445 \text{ in}^3$
Flow	$Q := \frac{d \cdot \omega}{2 \cdot \pi}$	$Q = 7.318 \text{ GPM}$	
Actual Specs	Actual Displacement	$d_a := .45 \text{ in}^3$	
	Actual Torque	$T_a := \frac{d_a \cdot p}{2 \cdot \pi} = 20.23 \text{ N}\cdot\text{r}$	
	Actual Flow	$Q_a := \frac{d_a \cdot \omega}{2 \cdot \pi} = 7.403 \text{ GPM}$	

Main Hydraulic Gear Pump Specs

Max Pressure	$p := 2500 \text{psi}$	$\text{psi} := \frac{\text{lbf}}{\text{in}^2}$	$\text{GPM} := \frac{\text{gal}}{\text{min}}$
Max Angular Velocity	$\omega := 3800 \text{rpm}$		
Displacement	$d := .45 \text{in}^3$		
Max Flow	$Q := \frac{d \cdot \omega}{2 \cdot \pi}$		
	$Q = 7.403 \text{GPM}$		
Maximum Torque	$T := \frac{d \cdot p}{2 \cdot \pi}$		
	$T = 20.23 \text{N} \cdot \text{m}$		
Max Power	$P := Q \cdot p$		
	$P = 8.05 \text{kW}$	$P = 10.795 \text{hp}$	

Electric Motor Specs

$$\omega_{ep} := 1725 \text{rpm}$$

$$P_{ep} := 1.5 \text{hp}$$

$$T_{ep} := \frac{P_{ep}}{\omega_{ep}} = 6.192 \text{N} \cdot \text{m}$$

Electrically Powered Pump

$Q_{ep} := 6.58 \text{GPM}$	Desired Flow
$p_{ep} := \frac{P_{ep}}{Q_{ep}} = 390.795 \text{psi}$	Max Pressure
$d_{ep} := 2 \frac{\pi \cdot Q_{ep}}{\omega_{ep}} = 0.881 \text{in}^3$	Designed Disp
$d_{ep} := .97 \text{in}^3$	Actual Disp
$Q_{ep} := \frac{d_{ep} \cdot \omega_{ep}}{2 \cdot \pi} = 7.244 \text{GPM}$	Actual Flow
$p_{ep} := \frac{P_{ep}}{Q_{ep}} = 354.998 \text{psi}$	Actual Max Pressure

Appendix B: Reservoir

Height: $h := 12\text{in}$ $V := 15\text{gal}$ $V = 56.78\text{L}$

Length: $l := 24\text{in}$

Width: $w := 12\text{in}$

$$V_2 := h \cdot l \cdot w = 56.634\text{L}$$

Wall thickness $t_r := .125\text{in}$ $t_r = 3.175\text{mm}$

$$A := 2 \cdot (l \cdot w) + 2 \cdot (h \cdot w) + 2 \cdot (l \cdot h)$$

Maximum temperature $T_i := 333\text{K}$ 140 degrees Fahrenheit

Maximum ambient air temperature $T_a := 310\text{K}$ 95 degrees Fahrenheit

Thermal conductivity of steel $K_A := \frac{43\text{ W}}{\text{m} \cdot \text{K}}$

Convective heat transfer coefficient of still air $h_c := 10 \frac{\text{W}}{\text{m}^2 \cdot \text{K}}$

Convective heat transfer coefficient of moving air $h_{c2} := 17 \frac{\text{W}}{\text{m}^2 \cdot \text{K}}$

Conductive resistance $R_1 := \frac{t_r}{K_A A}$

Convection resistance $R_2 := \frac{1}{h_c A}$

$$q_{\text{res}} := \frac{T_i - T_a}{R_1 + R_2} \quad q_{\text{res}} = 213.519\text{W}$$

The reservoir will not dissipate enough heat to keep the oil temperature below 140 degrees Fahrenheit and there for a heat exchanger will be necessary.

Appendix C: Heat Exchanger

Method 1

$$T_s := 333\text{K}$$

$$T_{\text{air}} := 310\text{K}$$

$$\text{Thickness of fin (assumed)} \quad t_f := 0.5\text{mm} \quad .027\text{in} = 0.686\text{mm}$$

Assuming circular fins:

$$\text{Inside radius (radius of tube)} \quad r_i := \frac{.375\text{in}}{2}$$

$$\text{Outside radius of fin} \quad r_o := r_i + .325\text{in}$$

$$\text{Parameter1} := \left(r_o - r_i + \frac{t_f}{2} \right)^{\frac{3}{2}} \cdot \left[\frac{2 \cdot h_{c2}}{K_A \cdot t_f \cdot (r_o - r_i)} \right]^{\frac{1}{2}} \quad \text{Parameter2} := \frac{\left(r_o + \frac{t_f}{2} \right)}{r_i}$$

$$\text{Parameter1} = 0.343$$

$$\text{Parameter2} = 2.786$$

Using the parameters and the graphs on page 103 of heat transfer text book the efficiency of a single fin can be found. It was estimated that the efficiency is 99% efficient.

$$n_{\text{fin}} := .99$$

$$\text{Heat dissipated by a single fin} \quad q_{\text{fin}} := n_{\text{fin}} \cdot h_{c2} \cdot 2 \cdot \pi \cdot \left[\left(r_o + \frac{t_f}{2} \right)^2 - r_i^2 \right] \cdot (T_s - T_{\text{air}})$$
$$q_{\text{fin}} = 0.35\text{W}$$

$$\text{Number of fins} \quad n := 2660$$

$$\text{Total heat dissipated by fins} \quad q_{\text{fintotal}} := q_{\text{fin}} \cdot n = 1.864\text{kW}$$

Calculating heat transferred by the remaining tube

Length of tube minus length covered by the fins.

$$l_t := 2 \cdot 20.25 \text{ in} - 2 \cdot 140 t_f = 0.889 \text{ m}$$

Tube diameter

$$d := \frac{3 \cdot \text{in}}{8}$$

Surface area of tube

$$A_t := \pi \cdot d \cdot l_t$$

Thermal Conductivity of Steel

$$K_s := \frac{43 \text{ W}}{\text{m} \cdot \text{K}}$$

Convective heat transfer coefficient of still air

$$h_{\text{sw}} := 10 \frac{\text{W}}{\text{m}^2 \cdot \text{K}}$$

Convective heat transfer coefficient of moving air

$$h_{\text{mw}} := 17 \frac{\text{W}}{\text{m}^2 \cdot \text{K}}$$

Conductive resistance

$$R_1 := \frac{t_f}{K_s A_t}$$

Convection resistance

$$R_2 := \frac{1}{h_c A_t}$$

Heat dissipate by one length of tubing

$$q_t := \frac{T_i - T_a}{R_1 + R_2} = 6.116 \text{ W}$$

Heat dissipated by entire tubing

$$q_{\text{ttotal}} := q_t \cdot 19 = 116.199 \text{ W}$$

Total heat dissipated by heat exchanger

$$q_{\text{he}} := q_{\text{fintotal}} + q_{\text{ttotal}} = 1.98 \times 10^3 \text{ W}$$

Heat dissipated by system

$$q_{\text{dis}} := q_{\text{he}} + q_{\text{res}} = 2.194 \times 10^3 \text{ W}$$

According to this calculation the heat exchanger will not dissipate enough heat through normal convection.

Method 2

Density of Oil $\rho := 875 \frac{\text{kg}}{\text{m}^3}$ $q_{\text{gen}} = 8.272 \times 10^3 \text{ W}$

Mass flow of oil $\dot{m} := Q_1 \cdot \rho = 0.35 \frac{\text{kg}}{\text{s}}$ $\text{kJ} := 1000\text{J}$

Specific heat of oil $C_p := 1.67 \frac{\text{kJ}}{\text{kg} \cdot \text{K}}$

Heat dissipated by 1 tube $\dot{q}_{\text{dis}} := \frac{q_{\text{gen}} - q_{\text{res}}}{19} = 424.13 \text{ W}$

Temperature of oil entering reservoir $T_i := 333 \text{ K}$

Temperature of oil exiting reservoir $T_o := \frac{-\dot{q}_{\text{dis}}}{\dot{m} \cdot C_p} + T_i = 332.274 \text{ K}$

Temperature Difference entering $\Delta T_a := T_i - T_{\text{air}}$

Temperature Difference exiting $\Delta T_b := T_o - T_{\text{air}}$

Log Mean Temperature difference $T_{\text{logmean}} := \frac{\Delta T_a - \Delta T_b}{\ln\left(\frac{\Delta T_a}{\Delta T_b}\right)} = 22.63 \text{ K}$

Area of 1 Fin $A_{1\text{fin}} := 2\pi\left(r_o^2 - r_i^2 + r_o \cdot t_f\right)$

Total area of fins $A_{\text{total}} := A_{1\text{fin}} \cdot 28$

Convective heat transfer coefficient $\dot{h} := \frac{\dot{q}_{\text{dis}}}{A_{\text{total}} \cdot T_{\text{logmean}}} = 69.484 \frac{\text{kg}}{\text{K} \cdot \text{s}^3}$

Thus, force convection heat transfer is necessary and normal convection heat transfer is not adequate.

Diameter of tube $D := \frac{3}{8} \text{ in}$

Prandelt Number $Pr := .71$

Note: Temperature of air is 310 K

Kinematic Viscosity of air $\nu := 8.32110^{-6} \frac{\text{m}^2}{\text{s}}$

Density of air $\rho_{\text{air}} := 1.7973 \frac{\text{kg}}{\text{m}^3}$

Specific heat of air $C_{\text{pair}} := 871 \cdot \frac{\text{J}}{\text{kg} \cdot \text{K}}$

Length of fin $L := 1 \cdot \text{in}$

Finding velocity of air

Guess

$$U_{\text{max}} := 4 \frac{\text{m}}{\text{s}}$$

Given

$$U_{\text{max}} = \left[\frac{\left(\frac{h_c \cdot Pr^3}{.930 \rho_{\text{air}} \cdot C_{\text{pair}} \cdot U_{\text{max}}} \right)^{-2} \cdot \nu}{L} \right]$$

$$U := \text{Find}(U_{\text{max}}) = 4.404 \frac{\text{m}}{\text{s}}$$

Sizing the Fan

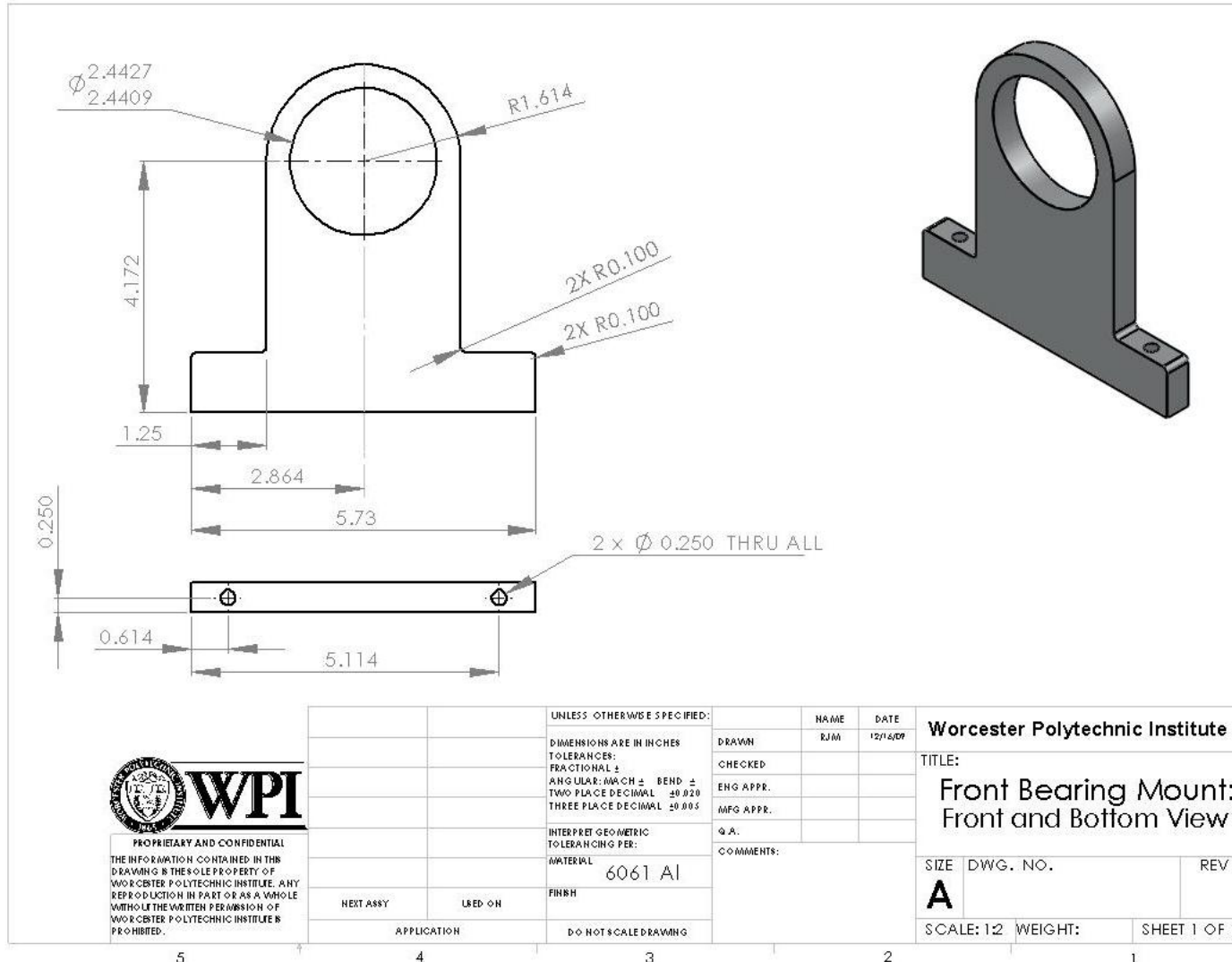
An AC axial fan blowing 1320 CFM and a fan hood 16in x 14in will produce an air speed of:

$$U_2 := 1320 \frac{\text{ft}^3}{\text{min}} = 0.623 \frac{\text{m}^3}{\text{s}}$$

$$U_v := \frac{U_2}{(14\text{in} \cdot 16\text{in})} = 4.311 \frac{\text{m}}{\text{s}}$$

Although this speed is slightly smaller than the required air speed. Other components will dissipate heat and therefore the heat exchnager will not have to dissipate all 8.5kW of heat produced.

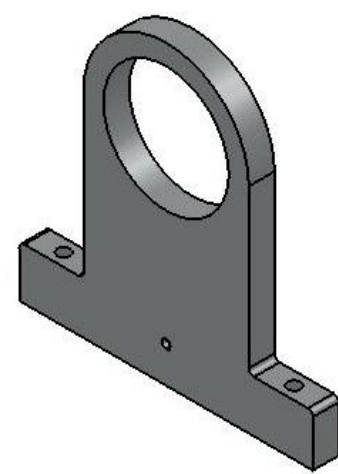
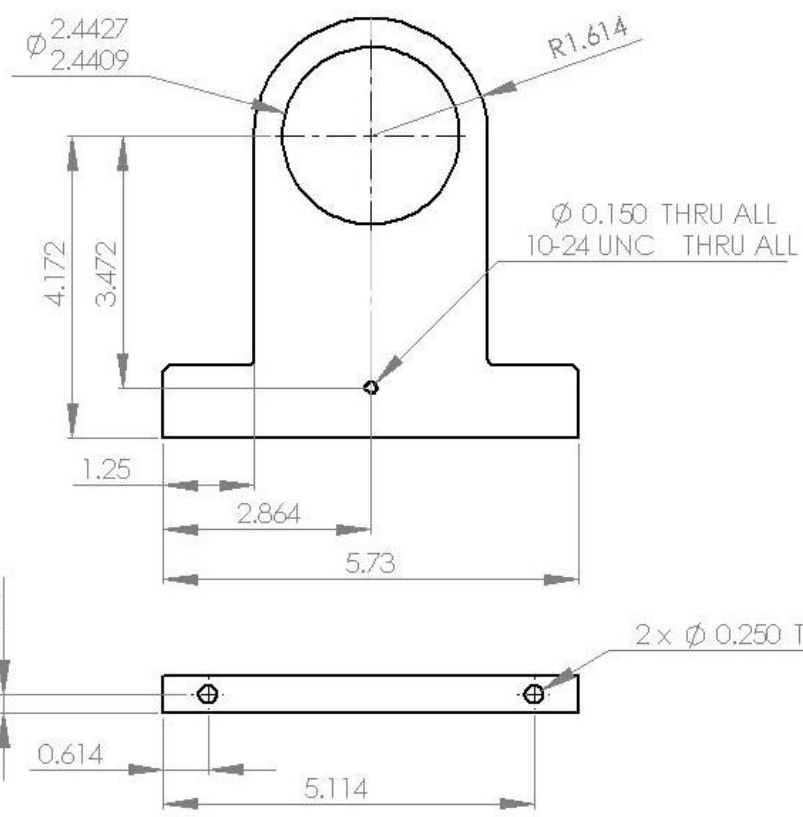
Appendix D: Cradle



PROPRIETARY AND CONFIDENTIAL
 THE INFORMATION CONTAINED IN THIS
 DRAWING IS THE SOLE PROPERTY OF
 WORCESTER POLYTECHNIC INSTITUTE. ANY
 REPRODUCTION IN PART OR AS A WHOLE
 WITHOUT THE WRITTEN PERMISSION OF
 WORCESTER POLYTECHNIC INSTITUTE IS
 PROHIBITED.

		UNLESS OTHERWISE SPECIFIED:		NAME	DATE
		DIMENSIONS ARE IN INCHES		DRAWN	RJM
		TOLERANCES:		CHECKED	
		FRACTIONAL \pm		ENG APPR.	
		ANGULAR: MACH \pm BEND \pm		MFG APPR.	
		TWO PLACE DECIMAL ± 0.020		Q.A.	
		THREE PLACE DECIMAL ± 0.005		COMMENTS:	
		INTERPRET GEOMETRIC TOLERANCING PER:			
		MATERIAL			
		6061 Al			
		FINISH			
		DO NOT SCALE DRAWING			
NEXT ASSY	USED ON				
APPLICATION					

Worcester Polytechnic Institute		
TITLE:		
Front Bearing Mount: Front and Bottom View		
SIZE	DWG. NO.	REV
A		
SCALE: 1:2	WEIGHT:	SHEET 1 OF 1

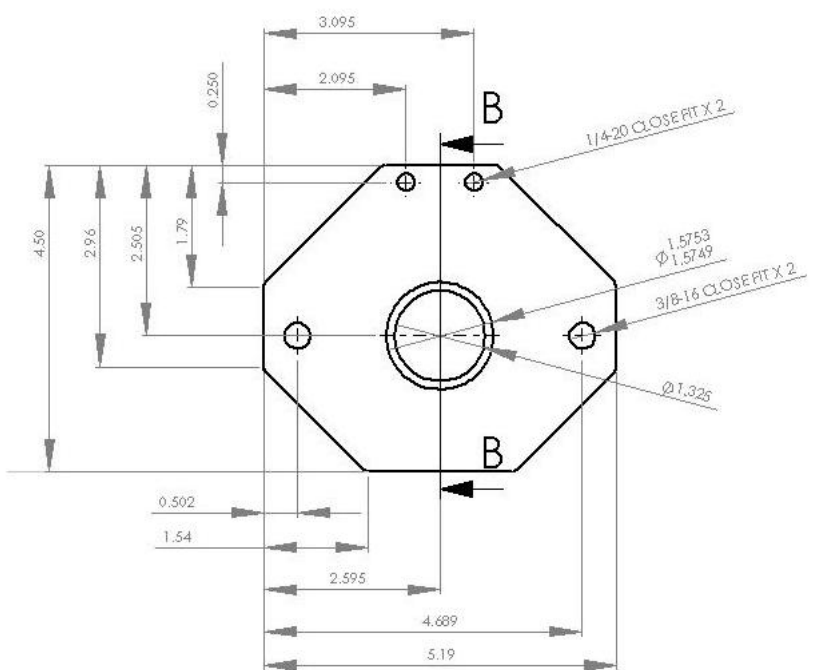


WPI
 PROPRIETARY AND CONFIDENTIAL
 THE INFORMATION CONTAINED IN THIS DRAWING IS THE SOLE PROPERTY OF WORCESTER POLYTECHNIC INSTITUTE. ANY REPRODUCTION IN PART OR AS A WHOLE WITHOUT THE WRITTEN PERMISSION OF WORCESTER POLYTECHNIC INSTITUTE IS PROHIBITED.

		UNLESS OTHERWISE SPECIFIED:	NAME	DATE
		DIMENSIONS ARE IN INCHES	DRAWN	RJM
		TO TOLERANCES:	CHECKED	12/16/09
		FRACTIONAL	ENG APPR.	
		ANGULAR: MACH ± BEND ±	MFG APPR.	
		TWO PLACE DECIMAL ±0.020	Q.A.	
		THREE PLACE DECIMAL ±0.005	COMMENTS:	
		INTERPRET GEOMETRIC TOLERANCING PER:		
		MATERIAL AL 6061		
		FINISH		
NEXT ASSY	USED ON	DO NOT SCALE DRAWING		
APPLICATION				

Worcester Polytechnic Institute		
TITLE:		
Rear Bearing Mount: Front and Bottom View		
SIZE	DWG. NO.	REV
A		
SCALE: 1:2	WEIGHT:	SHEET 1 OF 1

5 4 3 2 1



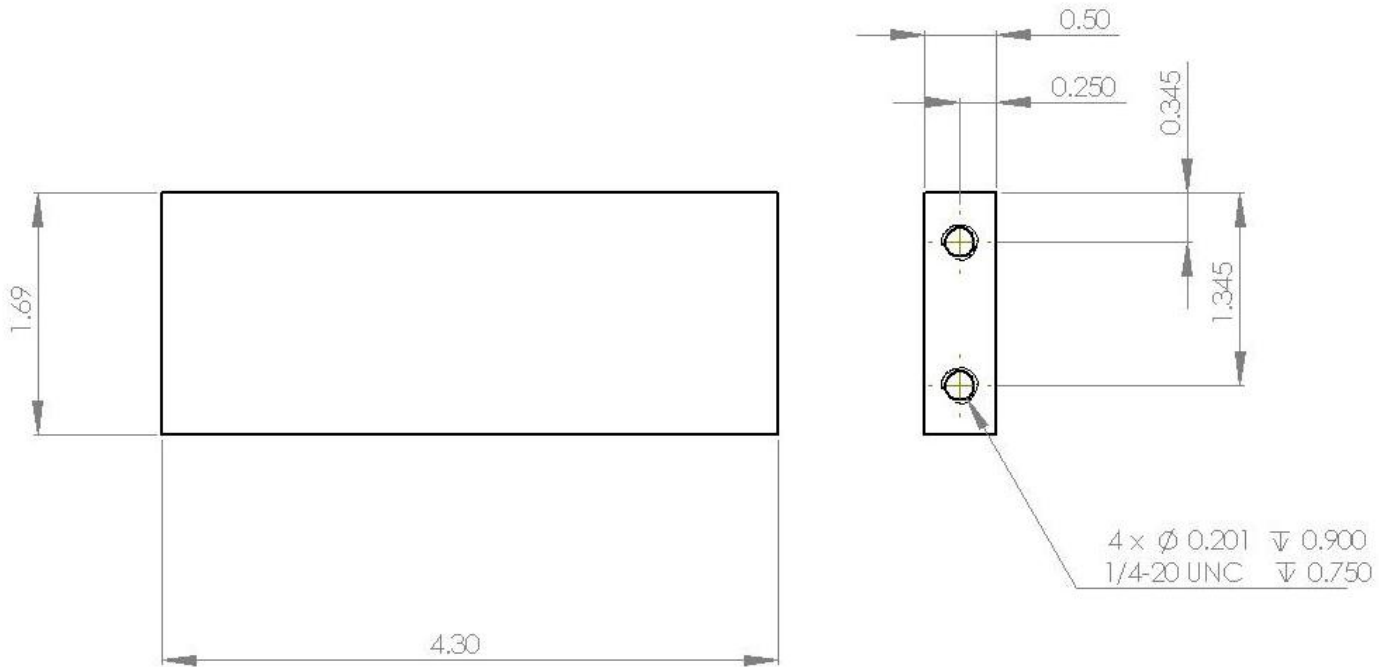
SECTION B-B
SCALE 1 : 2



PROPRIETARY AND CONFIDENTIAL
THE INFORMATION CONTAINED IN THIS DRAWING IS THE SOLE PROPERTY OF WORCESTER POLYTECHNIC INSTITUTE. ANY REPRODUCTION IN PART OR AS A WHOLE WITHOUT THE WRITTEN PERMISSION OF WORCESTER POLYTECHNIC INSTITUTE IS PROHIBITED.

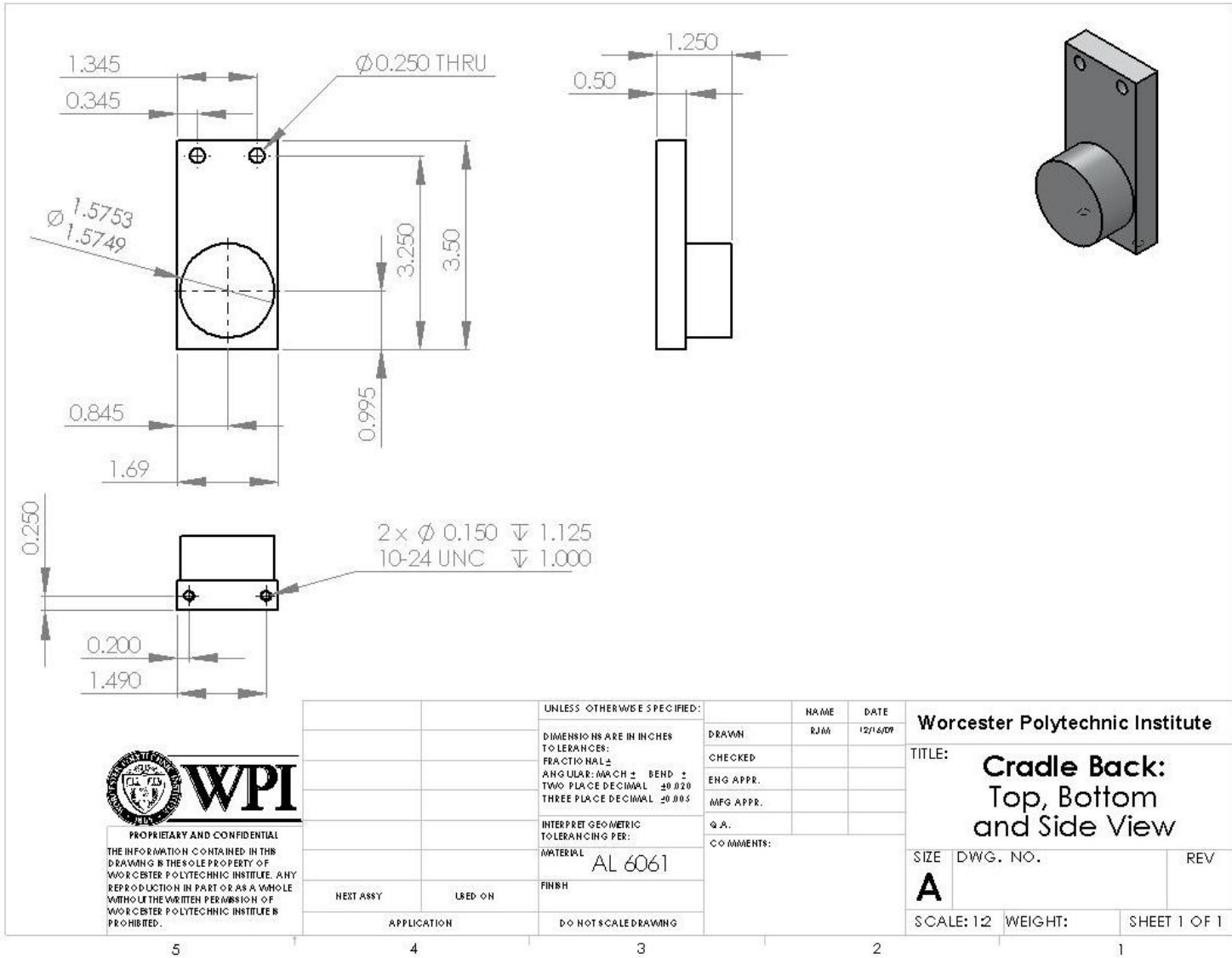
		UNLESS OTHERWISE SPECIFIED:	NAME	DATE	Worcester Polytechnic Institute	
		DIMENSIONS ARE IN INCHES	RJM	12/16/09	TITLE:	
		TOLERANCES:			Cradle Front:	
		FRACTIONAL ±			Front and Section View	
		ANGULAR MATCH ± BEND ±			SIZE	DWG. NO.
		TWO PLACE DECIMAL ±0.020			A	REV
		THREE PLACE DECIMAL ±0.005			SCALE: 1:2	WEIGHT:
		INTERPRET GEOMETRIC TOLERANCING PER:			SHEET 1 OF 1	
		MATERIAL				
		AL 6061				
		FINISH				
NEXT ASSY	USED ON	APPLICATION	DO NOT SCALE DRAWING			

5 4 3 2 1



PROPRIETARY AND CONFIDENTIAL
 THE INFORMATION CONTAINED IN THIS DRAWING IS THE SOLE PROPERTY OF WORCESTER POLYTECHNIC INSTITUTE. ANY REPRODUCTION IN PART OR AS A WHOLE WITHOUT THE WRITTEN PERMISSION OF WORCESTER POLYTECHNIC INSTITUTE IS PROHIBITED.

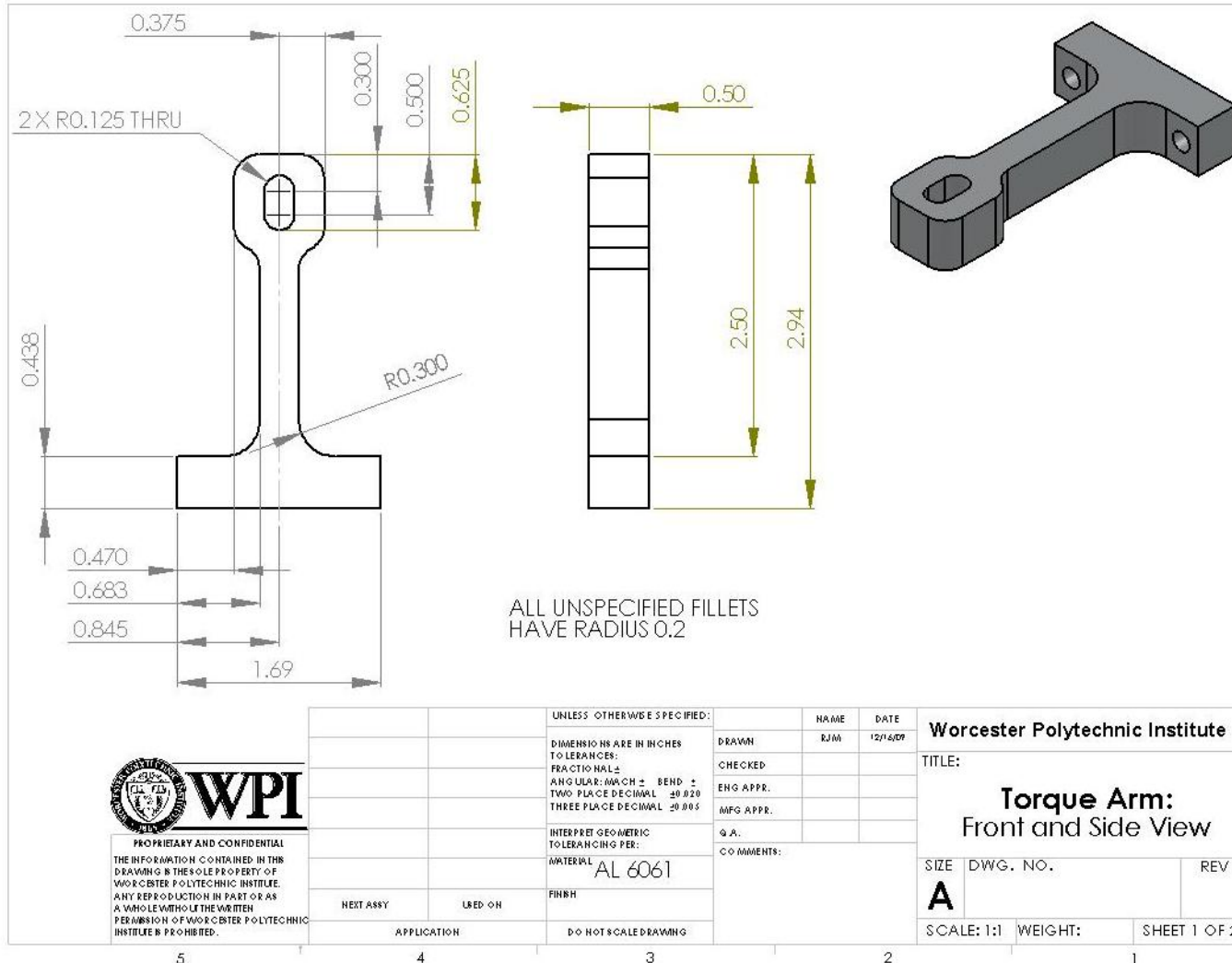
		UNLESS OTHERWISE SPECIFIED:		NAME	DATE	Worcester Polytechnic Institute	
		DIMENSIONS ARE IN INCHES TOLERANCES: FRACTIONAL ± ANGULAR: MACH ± BEND ± TWO PLACE DECIMAL ±0.020 THREE PLACE DECIMAL ±0.005		DRAWN	RJM	12/16/09	TITLE:
		INTERPRET GEOMETRIC TOLERANCING PER:		CHECKED			Cradle Middle: Top and Right Views
		MATERIAL AL 6061		ENG APPR.			SIZE DWG. NO.
NEXT ASSY		FINISH		MFG APPR.			REV
APPLICATION		DO NOT SCALE DRAWING		Q.A.			A
				COMMENTS: Right and Left Views are identical			SCALE: 1:1 WEIGHT: SHEET 1 OF 1
5	4	3	2	1			

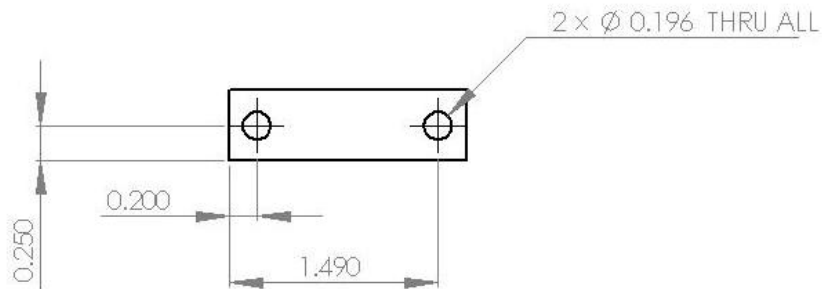


PROPRIETARY AND CONFIDENTIAL
 THE INFORMATION CONTAINED IN THIS DRAWING IS THE SOLE PROPERTY OF WORCESTER POLYTECHNIC INSTITUTE. ANY REPRODUCTION IN PART OR AS A WHOLE WITHOUT THE WRITTEN PERMISSION OF WORCESTER POLYTECHNIC INSTITUTE IS PROHIBITED.

UNLESS OTHERWISE SPECIFIED:		NAME	DATE	Worcester Polytechnic Institute
DIMENSIONS ARE IN INCHES		DRAWN	RJM	
TOLERANCES:		CHECKED		TITLE: Cradle Back: Top, Bottom and Side View
FRACTIONAL ±		ENG APPR.		
ANGULAR: HATCH ± BEND ±		MFG APPR.		
TWO PLACE DECIMAL ±0.020		Q.A.		SIZE DWG. NO.
THREE PLACE DECIMAL ±0.005		COMMENTS:		REV
INTERPRET GEOMETRIC TOLERANCING PER:				SCALE: 1:2 WEIGHT: SHEET 1 OF 1
MATERIAL AL 6061				
NEXT ASSY	USED ON	FINISH		
APPLICATION		DO NOT SCALE DRAWING		

Appendix E: Torque Arm





WPI
 PROPRIETARY AND CONFIDENTIAL
 THE INFORMATION CONTAINED IN THIS
 DRAWING IS THE SOLE PROPERTY OF
 WORCESTER POLYTECHNIC INSTITUTE. ANY
 REPRODUCTION IN PART OR AS A WHOLE
 WITHOUT THE WRITTEN PERMISSION OF
 WORCESTER POLYTECHNIC INSTITUTE IS
 PROHIBITED.

		UNLESS OTHERWISE SPECIFIED:	NAME	DATE	Worcester Polytechnic Institute	
		DIMENSIONS ARE IN INCHES	DRAWN	RJM	12/16/09	TITLE:
		TOLERANCES:	CHECKED			Torque Arm:
		FRACTIONAL ±	ENG APPR.			Bottom View
		ANGULAR: MACH ± BEND ±	MFG APPR.			SIZE DWG. NO. REV
		TWO PLACE DECIMAL ±0.020	QA			A
		THREE PLACE DECIMAL ±0.005	COMMENTS:			SCALE: 1:1 WEIGHT: SHEET 2 OF 2
		INTERPRET GEOMETRIC TOLERANCING PER:				
		MATERIAL				
		AL 6061				
NEXT ASSY	USED ON	FINISH				
APPLICATION		DO NOT SCALE DRAWING				

5

4

3

2

1

Appendix F: Stress Calculations

Inputs

$$T := 20\text{N}\cdot\text{m}$$

$$L := 3.47\text{m} \quad L = 0.088\text{m}$$

$$F := \frac{T}{L} \quad F = 226.917\text{N}$$

$$\sigma_{\text{yield}} := 276\text{MPa}$$

$$\sigma := \frac{\sigma_{\text{yield}}}{4} \quad \sigma = 69\text{MPa}$$

$$b := .5\text{m} \quad \text{Width}$$

$$h := .325\text{m} \quad \text{THICKNESS OF TORQUE ARM}$$

$$c := \frac{h}{2}$$

Equations

$$L_1 := 1.74\text{m} \quad \text{LENGTH TO CRITICAL SECTION}$$

$$M := F \cdot L_1 = 10.029\text{N}\cdot\text{m}$$

$$I_x := \frac{b \cdot h^3}{12}$$

$$\sigma_1 := \frac{M \cdot c}{I_x}$$

$$\sigma_1 = 69.529\text{MPa} \quad \text{STRESS ON BEAM WITH THICKNESS "h"}$$

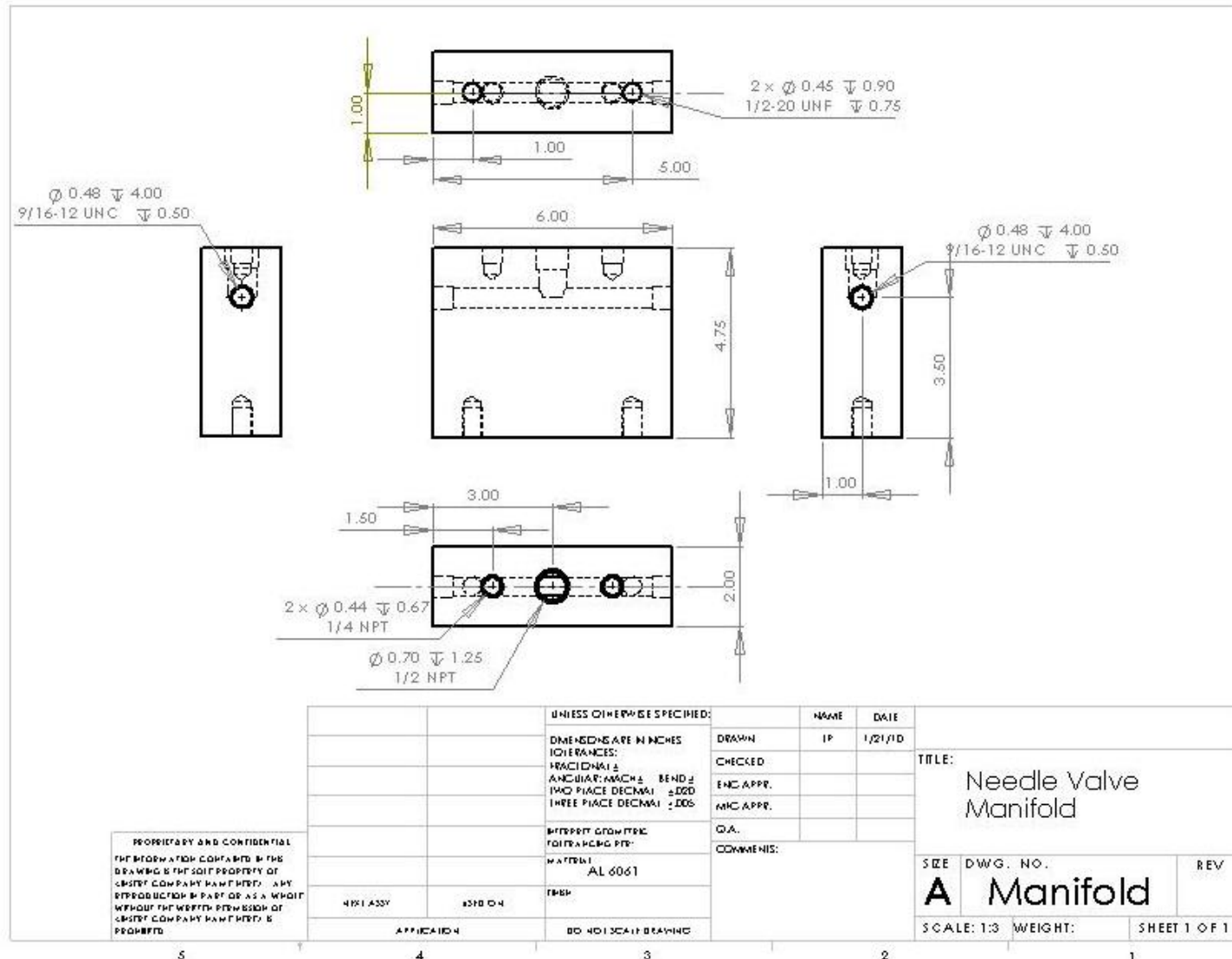
English

$$F = 51.013\text{bf}$$

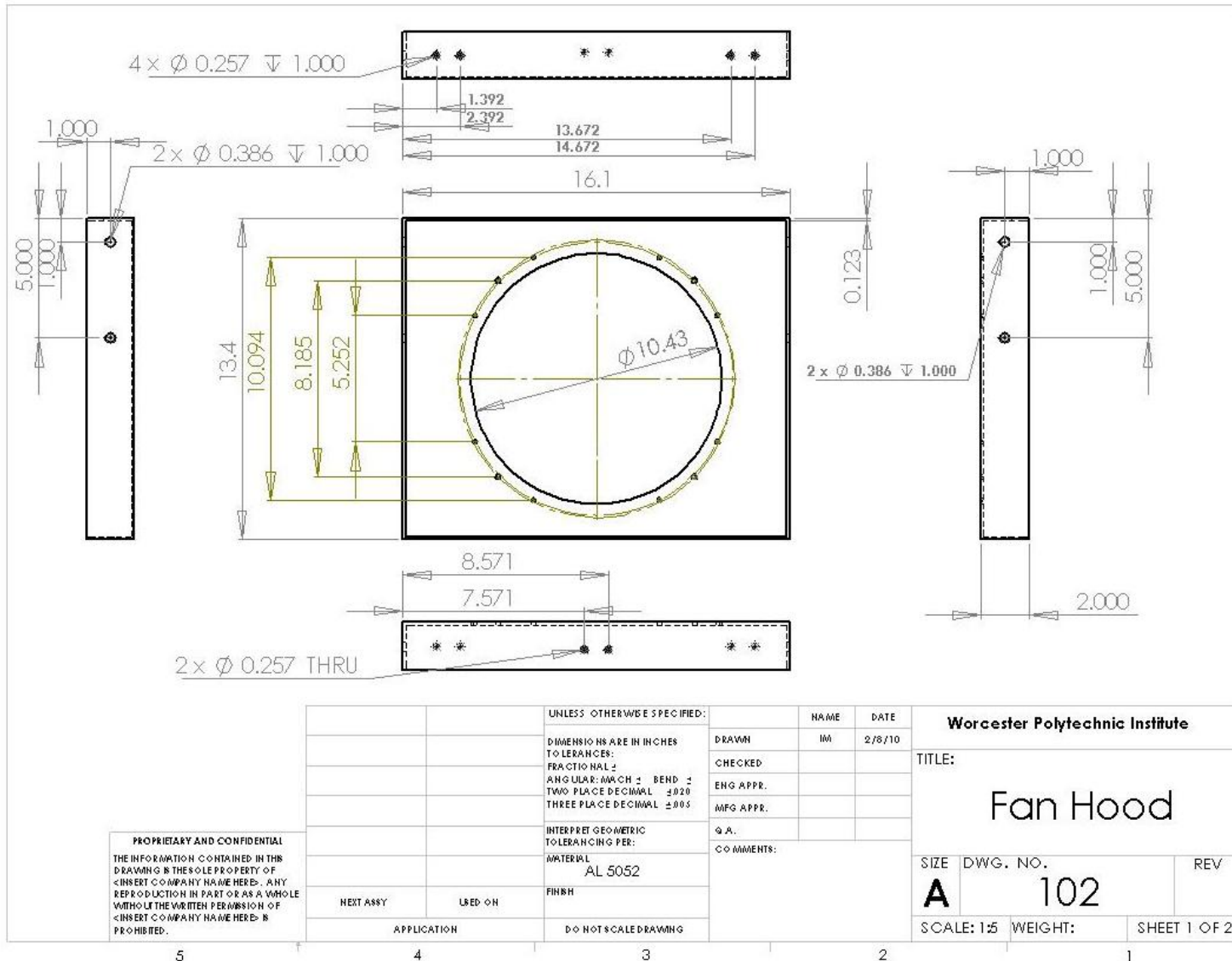
$$\sigma_1 = 10.084\text{ksi}$$

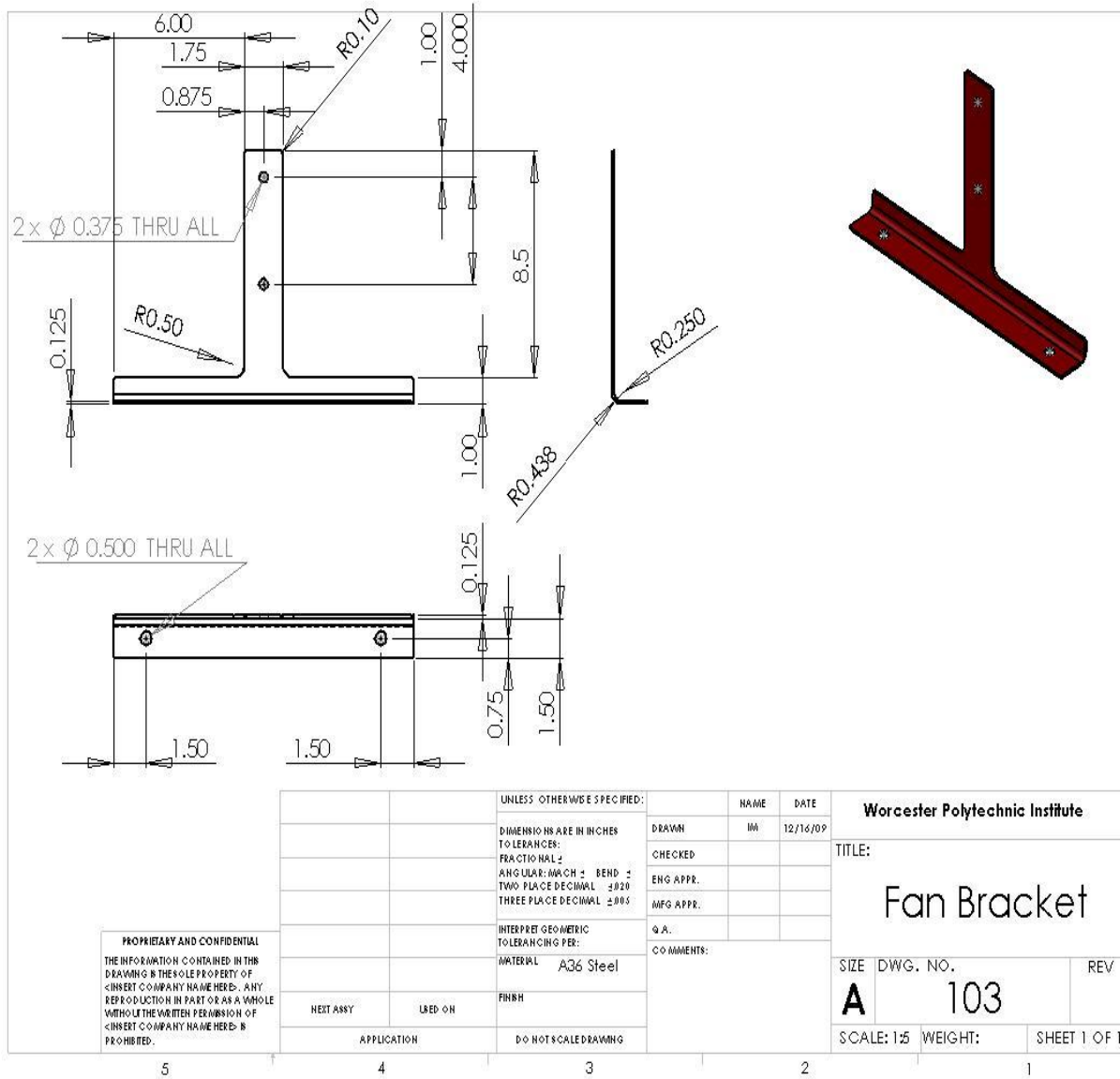
$$h = 0.325\text{in}$$

Appendix G: Manifold



Appendix H: Heat Exchanger

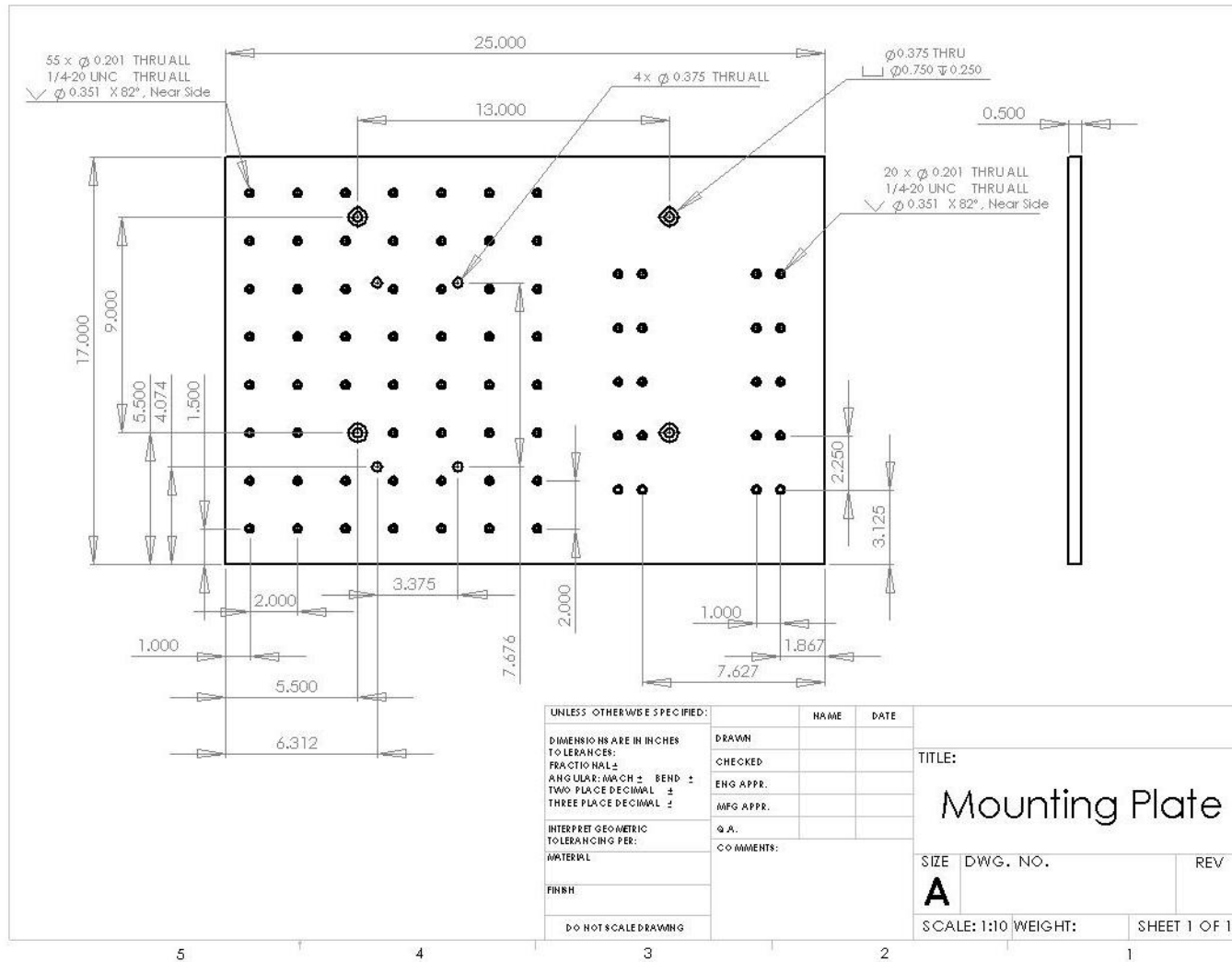




PROPRIETARY AND CONFIDENTIAL
 THE INFORMATION CONTAINED IN THIS DRAWING IS THE SOLE PROPERTY OF <INSERT COMPANY NAME HERE>. ANY REPRODUCTION IN PART OR AS A WHOLE WITHOUT THE WRITTEN PERMISSION OF <INSERT COMPANY NAME HERE> IS PROHIBITED.

		UNLESS OTHERWISE SPECIFIED:		NAME	DATE	Worcester Polytechnic Institute	
		DIMENSIONS ARE IN INCHES TO TOLERANCES:		DRAWN	MA	12/16/09	
		FRACTIONAL ±		CHECKED			TITLE:
		ANGULAR: MATCH ± BEND ±		ENG APPR.			Fan Bracket
		TWO PLACE DECIMAL ±0.01		MFG APPR.			
		THREE PLACE DECIMAL ±0.005		Q.A.			
		INTERPRET GEOMETRIC TOLERANCING PER:		COMMENTS:			
		MATERIAL: A36 Steel					SIZE DWG. NO. REV
		FINISH:					A 103
NEXT ANY	USED ON						SCALE: 1:5 WEIGHT: SHEET 1 OF 1
	APPLICATION	DO NOT SCALE DRAWING					

Appendix I: Base Plate



Appendix J: Strain Gage Calibration

Using Torque & Moment Equations							
Force	Expected	Calculated	Relationship	Force	Expected	Calculated	Relationship
2	1.047	0.365	2.868493151	2	1.047	0.42	2.492857143
4	2.093	0.68	3.077941176	4	2.093	0.7	2.99
6	3.014	1.025	2.940487805	6	3.014	0.985	3.059898477
8	4.186	1.375	3.044363636	8	4.186	1.19	3.517647059
10	5.233	1.675	3.124179104	10	5.233	1.67	3.133532934

All	3.011092975
- Outliers	3.046742931
Error	2.453%

All	3.038787123
- Outliers	3.175269618
Error	-1.694%

Force	Expected	Calculated	Relationship
2	1.047	0.325	3.221538462
4	2.093	0.625	3.3488
6	3.014	0.965	3.123316062
8	4.186	1.32	3.171212121
10	5.233	1.825	2.86739726

Force	Expected	Calculated	Relationship
2	1.047	0.2925	3.579487179
4	2.093	0.662	3.16163142
6	3.014	0.985	3.059898477
8	4.186	1.2225	3.424130879
10	5.233	1.805	2.899168975

All	3.146452781
- Outliers	3.127681361
Error	-0.198%

All	3.224863386
- Outliers	3.136207438
Error	-0.470%

Relationship	3.121475337
Average Error	1.20%

Relating Voltage to Torque							
Force	Expected	Calculated	Relationship	Force	Expected	Calculated	Relationship
2	1.047	0.0001725	6069.565	2	1.047	0.00016	6543.750
4	2.093	0.00039	5366.667	4	2.093	0.000355	5895.775
6	3.014	0.000555	5430.631	6	3.014	0.000525	5740.952
8	4.186	0.000725	5773.793	8	4.186	0.000725	5773.793
10	5.233	0.000895	5846.927	10	5.233	0.000846	6185.579

All	5697.517
- Outliers	5604.504
Error	2.628%

All	6027.970
- Outliers	5899.025
Error	-2.496%

Force	Expected	Calculated	Relationship
2	1.047	0.000185	5659.459
4	2.093	0.000365	5734.247
6	3.014	0.000565	5334.513
8	4.186	0.00078	5366.667
10	5.233	0.000945	5537.566

Force	Expected	Calculated	Relationship
2	1.047	0.00016	6543.750
4	2.093	0.00034	6155.882
6	3.014	0.000549	5489.982
8	4.186	0.00069	6066.667
10	5.233	0.0009625	5436.883

All	5526.490
- Outliers	5493.248
Error	4.706%

All	5938.633
- Outliers	5787.353
Error	-0.615%

Relationship	5751.764638
Average Error	2.61%

Relating Voltage to Torque -- With 84.9 Gain (100K/1K)							
Force	Expected	Calculated	Relationship	Force	Expected	Calculated	Relationship
2	1.047	0.0224	46.741	2	1.047	0.0176	59.489
4	2.093	0.03765	55.591	4	2.093	0.0369	56.721
6	3.014	0.0552	54.601	6	3.014	0.0575	52.417
8	4.186	0.07675	54.541	8	4.186	0.0765	54.719
10	5.233	0.09375	55.819	10	5.233	0.09175	57.035

All	53.459
- Outliers	55.138
Error	0.077%

All	56.076
- Outliers	55.223
Error	-0.077%

Force	Expected	Calculated	Relationship
2	1.047	0.0213	49.155
4	2.093	0.0397	52.720
6	3.014	0.0566	53.251
8	4.186	0.0753	55.591
10	5.233	0.0935	55.968

Force	Expected	Calculated	Relationship
2	1.047	0.0176	59.489
4	2.093	0.0361	57.978
6	3.014	0.055	54.800
8	4.186	0.075	55.813
10	5.233	0.092	56.880

All	53.337
- Outliers	54.383
Error	1.467%

All	56.992
- Outliers	56.368
Error	-2.106%

Relationship	55.1805464
Average Error	0.93%

Relating Voltage to Torque -- With 84.9 Gain (100K/1K)							
Force	Expected	Calculated	Relationship	Force	Expected	Calculated	Relationship
2	1.047	0.91	1.151	2	1.047	1	1.047
4	2.093	2.035	1.029	4	2.093	2.06	1.016
6	3.014	2.95	1.022	6	3.014	3	1.005
8	4.186	3.94	1.062	8	4.186	3.96	1.057
10	5.233	5.025	1.041	10	5.233	5.15	1.016

All	1.061
- Outliers	1.039
Error	-0.724%

All	1.028
- Outliers	1.023
Error	0.735%

Force	Expected	Calculated	Relationship
2	1.047	1.07	0.979
4	2.093	2.18	0.960
6	3.014	3.265	0.923
8	4.186	4.15	1.009
10	5.233	5.2	1.006

All	0.975
- Outliers	0.975
Error	5.790%

Relationship	1.030987378
Average Error	2.42%

Appendix K: Results

